THESIS FOR THE DEGREE OF DOCTOR OF PHILOSOPHY

Aspects of Efficient Parameter Estimation for Diesel Oxidation Catalysts

BJÖRN LUNDBERG

Division of Chemical Engineering
Department of Chemistry and Chemical Engineering
CHALMERS UNIVERSITY OF TECHNOLOGY
Göteborg, Sweden 2015

Aspects of Efficient Parameter Estimation for Diesel Oxidation Catalysts
BJÖRN LUNDBERG

Doktorsavhandling vid Chalmers tekniska högskola
Serie nr 2015: 3852
ISBN: 978-91-7597-171-1

Department of Chemistry and Chemical Engineering
Chalmers University of Technology
SE-412 96 Göteborg
Sweden
Telephone: +46(0)31-7721000

Cover Image: Full scale DOC with markings for insertion of thermocouples. Picture taken by Johnson Matthey. Edited by Fredrik Lundberg

Chalmers Reproservice
Göteborg, Sweden 2015

ASPECTS OF EFFICIENT PARAMETER ESTIMATION FOR DIESEL OXIDATION CATALYSTS

Björn Lundberg
Department of Chemistry and Chemical Engineering
Chalmers University of Technology
SE-412 96 Göteborg, Sweden

ABSTRACT

In this thesis the objective was to tune the model parameters of diesel oxidation catalysts (DOC) to measurement data from engine rig experiments in an efficient manner. The scope was however not limited to the algorithm of parameter search alone but instead included the whole process starting with the design of experiments.

Different aspects of efficient parameter estimation of a full scale DOC were evaluated. This included different kinetic models, mass transfer resistance evaluation, experiments at both engine rig and lab-scale, and parameter estimation algorithms. A specially developed detailed kinetic model, a method for parameter estimation using Multivariate Data Analysis, and a method for full scale engine rig experiments were all important products. In addition to these outputs some relevant conclusions were made based on the studies

- Including internal mass transport parameter in the tuning improved the possibilities of achieving a good fit for the catalyst model
- If internal mass transport is to be modeled the kinetic model cannot include parameters mimicking the effects of transport resistance
- A detailed kinetic model improves the conditions for separating kinetics and mass transport but also increases the need for experimental diversity at the same time as model instability may increase

Keywords: Exhaust Aftertreatment Modeling, DOC, Full Scale, Design of Experiments, Parameter Estimation, Engine Test Bench, MVDA, Kinetic Modeling, Mass Transport Modeling

ACKNOWLEDGEMENTS

I would like to take this opportunity to express my gratitude to all of those who helped me finish writing this thesis.

First I would like to thank all of my supervisors and Professor Bengt Andersson for giving me the opportunity to do my PhD at Chalmers in this interesting field of research. I would like to thank my supervisors at Chalmers, Professor Derek Creaser and Docent Jonas Sjöblom, for always encouraging me and for many rewarding discussions. Every time I've thought I've reached a dead end you have helped me find a new path to explore, your guidance has been invaluable. I would also like to thank my industrial partners Johnson Matthey and Scania AB, and in specific my industrial supervisors Dr. Åsa Johansson and Dr. Björn Westerberg. Thanks for valuable input and discussions during our monthly meetings and for making me feel welcome during my visits in Högsbo and Södertälje. Special thanks to Björn and Scania AB for allowing me to publish the engine rig set-up of their design in Paper IV.

I would like to thank all present and former colleagues at the Division of Chemical Engineering for a relaxed atmosphere and for enjoyable discussions, both work related and not. Sometimes I feel very lucky to have colleagues who drop by my office and make me forget about my work from time to time, I could thank you all by names but you all know who you are.

Financial support from Swedish Energy Agency and from ÅForsk is gratefully acknowledged. Also thanks to Swedish National Infrastructure for Computing (SNIC) at C3SE for the computational resources used in this project.

I would like to thank my friends and family for being there and supporting me and for reminding me that there are more important things in life than work. Finally, I would like to thank Mikaela for all your patience and encouragement during this last year of my PhD. I look forward to all the time we'll spend together now that this thesis is finally printed.

LIST OF PUBLICATIONS

This thesis is based on the following enclosed papers

I **Parameter Estimation of a DOC from Engine Rig Experiments with a Discretized Catalyst Washcoat Model**
Björn Lundberg, Jonas Sjöblom, Åsa Johansson, Björn Westerberg and Derek Creaser (2014)
SAE Int. J. Engines 7(2): 1093-1112.

II **Model-based experimental screening for DOC parameter estimation**
Björn Lundberg, Jonas Sjöblom, Åsa Johansson, Björn Westerberg and Derek Creaser (2015)
Computers & Chemical Engineering 74(0): 144-157.

III **Catalyst Modeling Combining Kinetics and Mass Transfer Using an Inert Washcoat**
Björn Lundberg, Jonas Sjöblom, Åsa Johansson, Björn Westerberg and Derek Creaser
Manuscript

IV **New Methodology for Transient Engine Rig Experiments for Efficient Parameter Estimation**
Björn Lundberg, Jonas Sjöblom, Åsa Johansson, Björn Westerberg and Derek Creaser (2013)
SAE Int. J. Engines 6(4): 1995-2003.

The following papers have not been included in the thesis:

Modeling Study of 5 kWe-scale Autothermal Diesel Fuel Reformer
Derek Creaser, Karatzas Xanthias, Björn Lundberg, Lars Pettersson and Jazaer Dawody (2011)
Applied Catalysis A: General 404(1–2): 129-140.

Characterization of Particulate Matter from Direct Injected Gasoline Engines

Carolin Wang-Hansen, Per Ericsson, Björn Lundberg, Magnus Skoglundh, Per-Anders Carlsson and Bengt Andersson (2013) *Topics in catalysis 56: 446-451.*

Chromatographic separation of wood model constituents - Analysis and modeling of competing adsorption

Niklas Westerberg, Björn Lundberg, Anders Rasmuson

Submitted to: *Chemical Engineering Research and Design*

CONTRIBUTION REPORT

Paper I-III: Responsible for writing, planning and supervising experiments, data analysis and computation

Paper IV: Responsible for writing, planning and supervising experiments, data analysis and computation. Design of experimental set-up by Björn Westerberg.

TABLE OF CONTENTS

1 INTRODUCTION

1.1 HEAVY DUTY DIESEL ENGINES ENVIRONMENTAL ISSUES

The complete combustion of fossil fuel and air results in emission of CO_2 and H_2O. However the combustion in heavy duty diesel (HDD) engines, and other internal combustion engines, will never be complete which leads to the formation of CO, un-burnt hydrocarbons (HC), and also particulate matter such as soot in addition to CO_2 and H_2O [1]. The high temperatures in the engine during combustion will also lead to the formation of nitrogen oxides from oxygen and nitrogen in the intake air [2].

All of CO, CO_2, HC, NO_x, and particulate matter are major contributors to air pollution and in today's cars and trucks all of them except CO_2 are reduced in the after treatment system. The environmental issues associated with diesel engine exhaust are both numerous and diverse. CO poisoning is the most common type of fatal air poisoning worldwide [3] as it, even in small concentration, can severely hinder the delivery of oxygen to organs and tissues [4]. NO_x contributes to the acidification of land and lakes [5], has toxic effects on the respiratory system and can also in combination with HC produce ground level ozone [3]. Some of the different hydrocarbons produced by combustion are also considered carcinogenic to humans [6]. Exposure to urban particulate matter can lead to increased risk of a variety of respiratory diseases and adverse health effects such as lung cancer, bronchitis and asthma [7].

The current European emission standard for HDD, which regulates emissions of CO, HC, NO_x, and particulate matter, is called Euro VI and was introduced in 2013. Neither date nor details of the next upcoming European

emission standard are yet defined but the new limitations will with certainty further increase the need for the understanding of the aftertreatment system.

1.2 HETEROGENEOUS CATALYSIS

The common structure of a catalyst in the automotive industry is a monolith of flow through type with a shape that is generally cylindrical with quadratic channels, see figure 1. The catalyst can be divided into two parts; the porous washcoat that carries the active material where the reaction takes place (B in figure 1) and the solid substrate that gives the catalyst its' structure (A in figure 1). The substrates in the current study were made of cordierite that is a ceramic material with low density (ca 400 kg/m^3), high heat conduction and stable thermal properties [8]. To attain an efficient mass and heat transfer between the gas phase (exhaust gas) and solid phase (the washcoat) a large interfacial area is favorable. This is achieved by making the number of channels per catalyst cross sectional area large and as an example all catalyst configurations used in the current study had 62 channels per cm^2 (400 cells per square inch, cpsi).

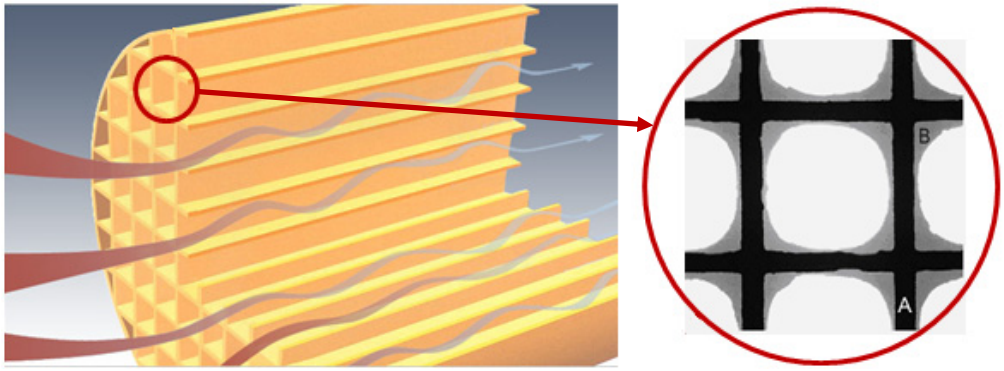

FIGURE 1 *Monolith and washcoat [9]*

The washcoat is coated on the inside of the walls of the substrate and forms a thin porous layer through which the exhaust needs to diffuse to react with the active material. Again to attain a high interfacial area between the exhaust gas diffusing through the washcoat and the active material, a large washcoat area per washcoat volume is desirable. High surface area materials such as γ-alumina are therefore commonly used as the primary washcoat material for oxidation catalysts. The active material is often a noble metal such as platinum or palladium.

1.2.1 MODELING SCALES

A full scale catalyst monolith is a highly dynamic system where different phenomena at several different length scales must be taken into account, see figure 2. At the largest scale a full scale catalyst of a HDD has length and diameter in the size range of decimeters and contains several thousands of channels. Inside the channels, that have an inside diameter of about a millimeter, heat and mass is transferred between the gas phase and the washcoat surface. The rate of transfer depends on several different variables such as the flow rate, composition and temperature in the gas phase, and composition and temperature at the washcoat surface. The catalyst washcoat is highly porous with pore sizes ranging from macropores of the order of 100 nm down to micropores of the order of 5-10 nm [10].

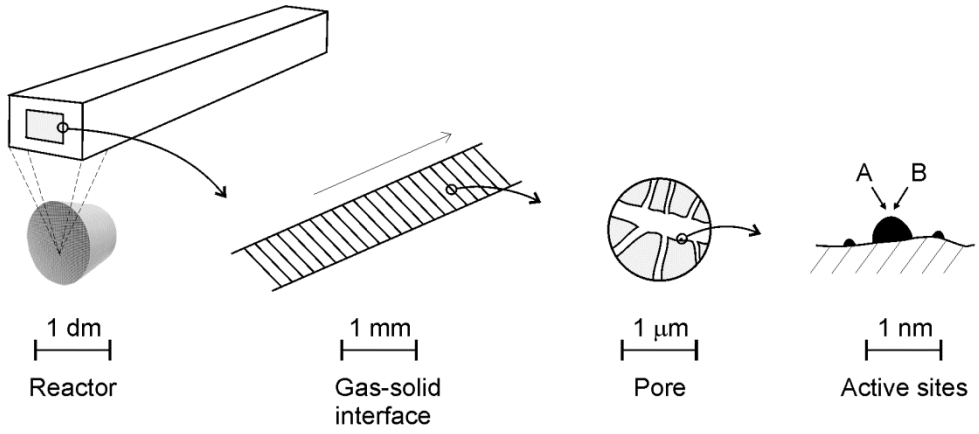

FIGURE 2 *Scales of heat and mass transport in full scale catalyst.*

The active material is finely dispersed on the pore walls as small clusters of atoms that contain the active sites. For a catalyzed reaction to take place at least one reacting molecule must chemisorb on an active surface. The rate of the chemisorption is governed by the properties of the adsorbing molecule and is also affected by the availability of vacant active sites. After a reaction has finally taken place on the active sites the product may desorb from the site and be transported back to the gas bulk.

Depending on the conditions, both the transport of reactants to the active sites and the reactions taking place on the active sites may limit the conversion over the catalyst. To model a full scale catalyst both kinetics, and heat and mass transfer therefore need to be taken into consideration.

1.3 THE ROLE OF THE DOC IN THE AFTERTREATMENT SYSTEM

The diesel oxidation catalyst (DOC) is a well established technology to reduce CO and hydrocarbon (HC) emissions from diesel engines that has been in use since the 1970s. Strengthened emission standards have made the importance of the DOC even greater in recent years since it has become an indispensible component for enhancing the performance of diesel particulate filters (DPF) and selective catalytic reduction (SCR) catalysts by utilization of oxidation of NO to NO_2.

Three reactions are desirable in the DOC; the oxidation of CO to CO_2, the oxidation of HC to CO_2 and the oxidation of NO to NO_2. In other words, the DOC does not remove NO_x but adjusts the NO_2/NO_x ratio which is important later in the aftertreatment system.

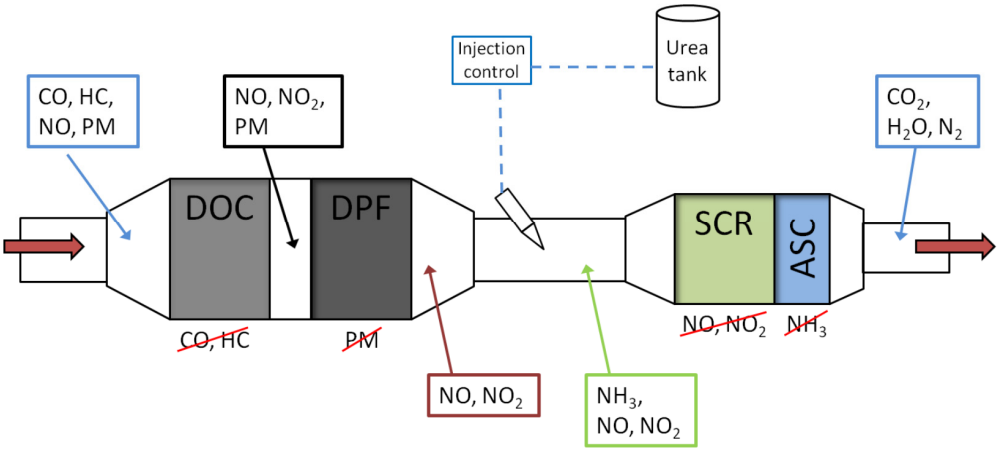

FIGURE 3 *Typical layout of an aftertreatment system used for heavy duty diesel vehicles [11]*

Figure 3 shows a typical layout of an aftertreatment system used for heavy duty diesel vehicles based on urea-SCR for controlling NO_x emissions. At ideal conditions both HC and CO have been fully oxidized in the DOC and the only pollutants left are NO_x and particulate matter (PM). The PM is trapped by the DPF and depending on if the DPF is passively or actively regenerated (PM oxidation) the DOC plays different roles. If active DPF regeneration is used the temperature will be periodically increased so that PM can be reduced by O_2, [12]. In this case the DOC is used to combust the temporarily increased HC content which generates the temperature increase. If passive DPF

regeneration is used, on the other hand, the DOC will be needed to provide NO_2 that enables PM oxidation at lower temperatures [12]. In fuel efficiency perspective the passive DPF is preferable since extra fuel injection is needed to perform the active DPF regeneration.

In the SCR, NO_x will be reduced to N_2 with NH_3 from the decomposition of injected urea. The desirable reaction here is the so called fast SCR reaction where equal amounts of NO and NO_2 are consumed [13]. The reactions in the SCR will therefore be dependent on the NO_2/NO_x fraction out from the DOC. The final component in the depicted aftertreatment system in figure 3 is the ammonia slip catalyst (ASC). The ASC reduces NH_3 that was not consumed in the SCR catalyst to N_2 and NO_x where N_2 is the preferred product.

It can be speculated that future legislations will also include CO_2 limits [14]. This may make a more complete combustion in the engine necessary which will increase the production of NO_x further and thereby increase the demand for NO_x reduction in the aftertreatment system. To conclude the DOC is an integral part of the aftertreatment system today and will with certainty continue to be so in the future.

1.4 OBJECTIVES

As the title of this thesis indicates the objective was to tune the model parameters of a DOC to measurement data in an efficient manner. The scope is however not limited to the algorithm of parameter search alone but instead includes the whole process starting with the design of experiments.

The design of experiments should be carried out in a manner in which the total experimental time is low (since especially engine rig experiments are very costly to perform) but at the same time the generated experimental data should be information rich and make it possible to estimate parameters as accurately as possible. This means that both the conditions of the gas reaching the catalyst and what catalyst configurations are used are of highest importance. To perform parameter estimation a suitable catalyst model is of course essential. The model used needs to be detailed enough to describe the reactions and transport phenomena in a full scale catalyst but it should at the same time be robust and simple to avoid too long simulation times. To find a good trade-off between model accuracy and computational time is therefore

an important part of the objective. This does not only include the model definition but also extends to the parameter search algorithm and utilization of computational resources. It should however not be forgotten that the most important objective is improved understanding of the process of parameter estimation where a good fit to measurement data is an indication of the applicability of the evaluated methods.

1.5 METHOD OVERVIEW

Two different approaches for efficient parameter estimation of a full scale DOC were evaluated. The two approaches have several features in common but differ in experimental complexity and in detail of the kinetic model. The first approach used only full scale experiments from a standard engine rig and a global kinetic model whereas the second approach used both lab-scale and full scale experiments and a detailed kinetic model. The first approach will therefore be denoted the *Engine rig only approach* throughout this dissertation and the second approach will be denoted the *Multi-scale experimental approach*. In many ways the second approach is an attempt to build on the conclusions from the first approach but it is also more complex and includes a wider set of experimental conditions at different scales. The suitability of the two approaches is therefore a function of the resources at hand as well as the detail level of the modeling.

1.5.1 THE ENGINE RIG ONLY APPROACH

To estimate kinetic parameters and to develop kinetic model structures, laboratory scale experimental data is generally used [15]. In laboratory scale it is possible to use essentially any combination of exhaust gas composition and temperature which makes it possible to estimate parameters over a wide range of conditions. However the validity of these parameters in full scale models is often limited and therefore the parameters commonly need to be re-tuned. It is this re-tuning of parameter values from lab-scale to full scale that was the aim with the first approach and therefore experiments were performed only in a standard engine rig.

The method can be summed up in four items

1. Design of Experiments (DoE)
2. Engine rig experiments
3. Multivariate data analysis (MVDA)
4. Parameter estimation

Items 1, 2 and 4 were applied in the first parameter estimation performed in Paper I and was extended with MVDA (item 3) in Paper II. Paper I can, in a sense, be viewed as a reference to how parameter estimation is normally performed and Paper II was an attempt to improve it. The full method therefore includes all four points even though they have not been applied in all of the parameter estimation performed in these papers. All of the points will be discussed in detail in upcoming sections and this section will only give a brief introduction.

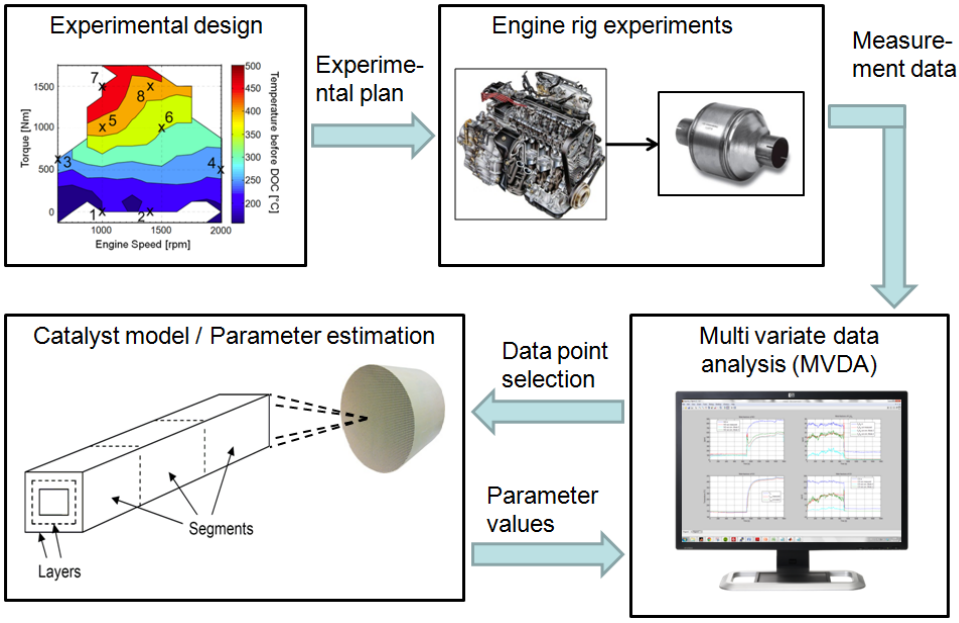

FIGURE 4 *Method overview of the Engine rig only approach*

The possible variation of the available variables (exhaust composition, flow, and temperature) of a full scale engine rig is severely limited by the operating points of the engine which is only governed by the engine torque and speed. The values of the different variables at different operating points are described by an engine map which also indicates what torque and speed combinations that are possible. To ensure that the variables are varied as much and as independently as possible an analysis of the map is performed. From this

analysis a set of suitable operating points are selected with Design of Experiments. To further increase the experimental space a number of different catalyst configurations were also used.

In item 2 the designed experiments are performed in an engine rig where the exhaust composition, flow, and temperature are measured before and after the catalyst. Item 3 and item 4 are strongly connected and the process after the experiments have been performed will here be described as a whole. In the traditional way of performing parameter estimation a gradient search method is used to minimize the residual sum square of all variables in all experimental data points. The method generally gives good results since all experimental data is used but there are some drawbacks such as, long simulation time, risk of finding a local minimum far from the global minima, risk of being dominated by certain parameters, and high parameter correlations. In the method presented in Paper II a balanced set of data points were selected for parameter estimation with the gradient search method. This aimed to give a more even influence on the residual from the estimated parameters and to reduce the risk of early convergence to a local minimum.

1.5.2 MULTI-SCALE EXPERIMENTAL APPROACH

The global kinetic model used in the first approach turned out to have parameters mimicking internal transport resistance which severely complicated the separation of mass transfer and kinetics. The parameters in question were part of an expression used in the global kinetic model to describe inhibition as a function of temperature and concentrations without modeling surface coverage. Improved conditions for modeling the distinction between kinetics and mass transport was therefore desirable to improve on the results from the first two studies (Paper I and II).

To generate good experimental data for modeling it is important to have measurements of both transient and stationary character. Due to the high thermal mass of an engine rig a change in engine loading point will generate transients lasting several minutes before a new stationary point is reached. It will thereby be time consuming to generate a wide range of different stationary points. Since experimental time was limited the diversity in the data generated from the engine rig in the Engine rig only approach was therefore not as high

as could be desired. A modified experimental method in full scale allowing more complex data to be generated was therefore identified as another potential improvement.

As a first step in the Multi-scale experimental method a pre-study in lab-scale was performed where a new kinetic model was constructed suitable for the application of full scale parameter estimation. The construction of the kinetic model included both deriving a model structure and estimating the parameters to lab-scale data. For the lab-scale study some of the catalysts were designed with an extra layer of inert washcoat to enhance the mass transport effects. This did not necessarily change the method presented in previous section but adds an input of a kinetic model to the inputs to the parameter estimation part.

To generate full scale data with faster transient the engine rig was expanded with some additional equipment allowing the inlet composition to the DOC to be changed without changing engine load point. This meant that the experimental design was no longer performed on only the engine map and catalyst configurations. Instead the new engine rig set-up allowed a switch of focus of the experimental plan from the engine to the control of the extra equipment between the engine and the catalyst to be modeled. A schematic overview of the Multi-scale experimental approach is given in figure 5.

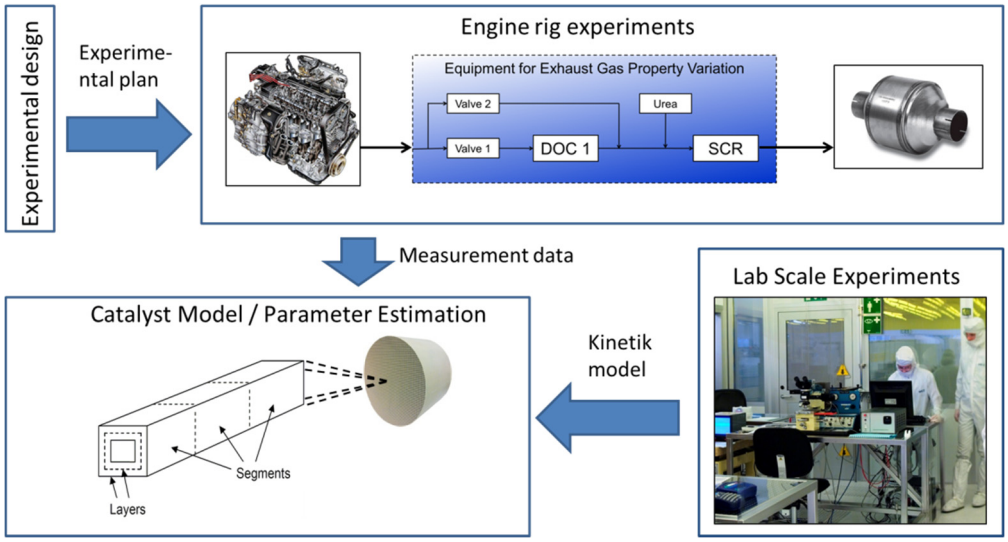

FIGURE 5 *Overview of Multi-scale experimental approach*

The Multi-scale experimental approach does not include MVDA as a part of the parameter estimation which should not be interpreted as an indication

of poor results when the algorithm was used. The reason for excluding MVDA will be discussed further in upcoming sections.

2 DESIGN OF EXPERIMENTS

Experimental design is a tool used to systematically examine the behavior and properties of a certain system that in the current case is a catalyst of DOC type. If the experiments are performed without structure the results will as well be unstructured and the analysis and eventual parameter estimation will be further complicated. Therefore a good experimental plan is the foundation of successful parameter estimation and should be thoroughly evaluated before any experiments are performed [16, 17].

A first important step in the experimental plan is to identify what variables can be investigated, what can be measured, and what the interesting responses are. For experimental measurements intended for catalyst modeling the gas composition, temperature and the flow rate both at the inlet and outlet should be monitored. The inlet conditions are changed by controlling equipment upstream of the catalyst such as the engine itself (Paper I, II and IV), a system of additional catalysts and valves (Paper IV) or individual mass flow controllers and heating (Paper III). For engine rig experiments there are more uncertainties and the catalyst inlet conditions should be measured but in the more controlled environment at lab-scale the system may be considered sufficiently well calibrated to follow a given set-point without being measured. Since the catalyst itself, which is to be modeled, has no influence on the inlet conditions all properties of the flow entering the catalyst must be variables. The outlet conditions on the other hand are a result of the catalyst performance and the response of the system is therefore the measured gas composition and temperature at the catalyst outlet. If the experiments would have been performed on a catalyst in powder form these variables and

responses may have been enough. In the current case significant mass transport resistance in the washcoat can, however, be expected which means that some variables should also be included that influence mass transport. The variables selected for this purpose in the current study are different catalyst configurations that will have different mass transfer properties.

In the simplest case all the variables can be varied independently and the model is linear and time independent. At lab-scale the first property is actually true but for a system as complex as the engine rig none of these properties are applicable. When the engine operating point (load and speed) is the only parameter to control the inlet properties, the variables will be highly correlated. A change in operating point will thereby more or less affect all of the variables (concentrations, flow rate, and temperature). A method of reducing these correlations is, however, presented in Paper IV. The catalyst is also a highly non-linear system which is easily deduced by only investigating some of the simplest kinetic models describing the DOC and becomes even more obvious when considering that mass and heat transport resistances may also influence its operation.

The large thermal mass of the catalyst also means that energy will be accumulated and thus the properties of the system will not only depend on the current inlet conditions but also on the inlet at earlier time points. For a full scale engine rig system this may be several minutes earlier if the temperature change is large. The temperature is however not the only variable with a dynamic behavior since also components can be accumulated in the washcoat as surface adsorbed species. Surface adsorbed species can generate dynamic behavior as a function of temperature, generally known as hysteresis, and will then give different reaction rates at identical inlet conditions as a result of different temperature history. The active sites may also be affected by more long term processes such as sintering and fouling.

The dynamic behavior of the system means that transient experiments are of outmost importance [18] and should be the central point of any experimental plan for catalyst systems. This is especially true since the system has unobservable variables such as quantities of surface adsorbed species.

Different types of transient experiments have been used in the current work and the first two studies were based solely on the simple step change in the engine operating point. Even these simple transients significantly increase the parameter sensitivity of the model and thereby improves the conditions for parameter estimation [19] compared to only using stationary data.

When input variables can be varied independently (applied to a linear model) it is possible to make an orthogonal design. In a system where the variables are inherently correlated the Design of Experiments should strive to make the design of experiments as orthogonal as possible. Also the parameters that are to be estimated may be correlated, this is however an issue that will be further discussed in sections 2.1 and 2.2.

2.1 PRINCIPAL COMPONENT ANALYSIS

Principal Component Analysis (PCA) is a mathematical method where large sets of observations of possibly correlated variables are transformed into new, linearly uncorrelated variables. The number of uncorrelated variables, usually referred to as principal components, can be chosen to be fewer or equal to the number of variables in the untreated data [20].

The PCA can be performed with several different purposes such as identification of classes of data and outliers, simplification, data reduction, variable selection, and prediction. A simple way of describing the method would be as an approximation of a data matrix where the more similarity within the objects result in fewer terms needed for a good fit.

In the first step of transforming a set of data (M) according to PCA the direction that captures the largest variation in the data is identified via least squares. The normalized vector describing the identified direction will be the first principal component in the transformed set of data (see figure 6). Another principal component can be added by again identifying the direction that captures the largest variation in the data but now with the added criterion that the direction must be orthogonal to the first principal component (see figure 6). Components are usually added to the PCA-model until the increase in information with the added component is below a certain limit. The matrix containing the principal component vectors is called the loadings vector and can be used to analyze the relation between variables.

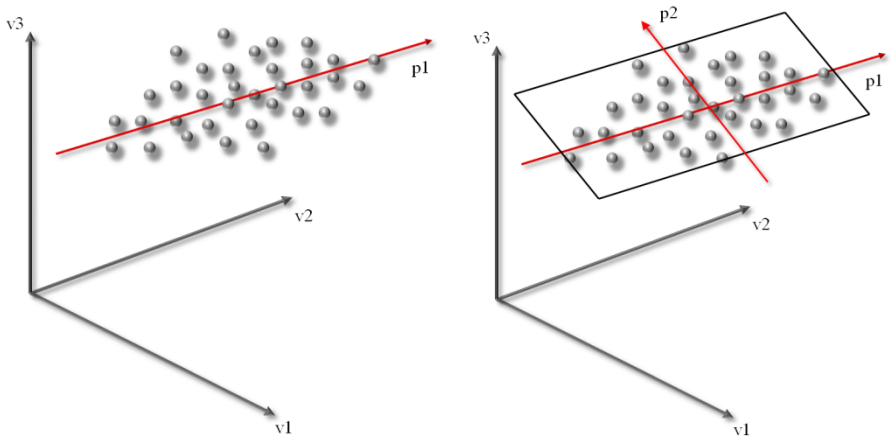

FIGURE 6 *First (left) and second (right) principal components of an arbitrary data set with three variables*

The observations (rows) are projected onto the sub-space defined by the principal components which will result in a number of vectors (as many as the number of principal components) that are orthogonal but not normalized. The vectors are summarized in the scores matrix that can be used to analyze the relations between observations.

In the current study PCA was used in Paper II to select the data points (observations) most suitable for parameter estimation which means that the scores matrix and not the loading matrix was the focus of the analysis.

The scores matrix and the loading matrix together form a linear combination to model the data matrix M (size N×K) according to

$$M = CL + E \quad (1)$$

where (for a PCA model with A components) C (size N×A) is the scores matrix, L (size A×K) is the loading matrix, and E is the error.

2.2 D-OPTIMAL DESIGN

For linear models traditional experimental designs such as full factorial designs, fractional factorial designs, and response surface designs are suitable when the factors are relatively unconstrained. For non-linear models such as a for a full scale catalyst, on the other hand, less traditional models such as D-optimal design may be more favorable.

If there would be restrictions on the number of experimental runs a full factorial design could be used as a candidate set for a D-optimal design to

create a new design matrix (M) with fewer rows (note that the candidate set can have several different origins, for example it could also be a large set of data where a high variable correlation has limited the available variable combinations). The D-optimal design algorithm would then in an iterative process select different combinations of rows from the candidate set that minimizes covariance of the new design matrix by maximizing the determinant of M^TM (hence the notation D-optimal as in determinant). This would maximize the orthogonality of the design matrix and as such create the design with the, in theory, best conditions for parameter estimation with the defined number of runs. Note that the iterative process in which D-optimal design is performed contains certain random factors which means that the D-optimal design performed on a large candidate set likely will generate different design matrices on different runs.

2.2.1 D-OPTIMAL ONION DESIGN

Since the D-optimal selection is using a linear model, the regular D-optimal design will result in a selection where only the most extreme points are chosen. These points will maximize the diversity of the design matrix, according to the description in previous section, but may not be representative for the whole data. If the points are time points used for parameter estimation the result could even be a sub-optimization of the residual over the entire data set. In a D-optimal onion design, introduced by Olsson et al. [21, 22], the data set is divided into layers where every layer includes points in a specified range (such as parameter sensitivity in Paper II). The D-optimal design is then applied to every onion layer and a number of data points will thereby be selected in every range, resulting in a more balanced data point selection.

3 EXPERIMENTAL

To use an engine as the exhaust source together with full scale catalysts results in comprehensive challenges for how the experiments should be performed. This is not only due to the fact that a full scale catalyst is a complex system but also because the engine itself severely limits the possibilities to vary the catalyst inlet conditions. In this section the different engine rig set-ups used in Paper I and II (section 3.2), and Paper IV (section 3.3) are introduced together with the possibilities for experimental design made available with these set-ups. Even though the focus of the current work was parameter estimation from full scale experiments some lab-scale experiments were also performed for detailed kinetic modeling. The lab-scale set-up together with a description of the performed experiments is given in section 3.4. The importance of the catalyst configurations as a part of the experimental design has already been mentioned and the catalyst configurations in all studies will therefore be introduced before the different experimental set-ups where they were used.

3.1 CATALYST CONFIGURATIONS

As mentioned in the previous section the experimental design does not only include how the inlet conditions to the catalyst are controlled, the design of the actual catalyst is also a very important part. Catalyst properties such as, noble metal loading, washcoat thickness, catalyst volume, active surface area, and transport resistance will influence the reactions taking place in the catalyst. To achieve a variation in these properties a number of different model catalysts were custom made for the project. The same set of catalyst was used for all full

scale experiments but for the lab-scale experiments a different design was used to enhance mass transport limitations.

3.1.1 FULL SCALE CONFIGURATIONS

The catalysts used were platinum only model catalysts of HDD dimensions and were provided by Johnson Matthey. The catalyst configurations are summarized in table 1.

TABLE 1 *Properties of full scale catalysts used in the project*

Configu-ration	**Pt-loading [g/ft^{3}monolith]**	**Length [cm]**	**Average washcoat thickness* [µm]**
a	15	10.2	110
b	30	10.2	110
c	15	2x10.2	110
d	15	10.2	55
e	5	10.2	110

*Washcoat thickness is generally higher in the corners of the channel and may also vary axially

Some catalysts were made with replicates making it possible to put them in series to allow catalyst configurations with increased catalyst volume and thereby also increased residence time for the exhaust in the catalyst. This possibility was used for catalyst configuration c in table 1 where two catalysts of configuration a were used in series. All catalysts were of monolith flow-through type with 62 square channels per cm^2 (400 cpsi), a total diameter of 30.5 cm (12 inch), and a total length of 10.2 cm (4 inch).

3.1.2 LAB-SCALE CONFIGURATIONS

To obtain a wide span of experimental data six different catalyst configurations with different platinum loadings and inert washcoat layer thicknesses were used. The purpose of the inert washcoat layer was to enhance mass transport resistance to improve the conditions for separating mass transport and kinetics in the model. All catalysts, shown in table 2, had an active washcoat loading of 1 g/inch^3, a monolith length and diameter of 1 inch and cell density of 400 cpsi. The catalysts were platinum only model catalysts provided by Johnson Matthey.

TABLE 2 *Properties of lab-scale catalysts used in the project*

ID#	Pt loading [g/ft^3]	Inert washcoat loading [g/inch^3]	Average inert washcoat thickness* [µm]	Average total washcoat thickness* [µm]
1	1	0	0	35
2	5	0	0	35
3	1	1	37	72
4	3	1	37	72
5	5	1	37	72
6	5	2	78	113

*Washcoat thickness is generally higher in the corners of the channel and may also vary axially

A visual display of the catalyst configurations are given in figure 7. The reason for only including one catalyst configuration with the highest inert washcoat loading was that conversions were assumed to be low for the selected experimental range for the lower platinum loadings of 1 g/ft^3 and 3 g/ft^3.

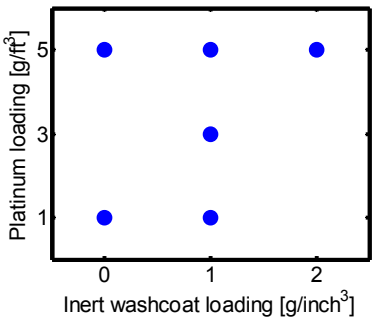

FIGURE 7 *Schematic description of catalyst configurations*

The lab-scale catalysts were samples taken from full scale catalysts produced specifically for the study. Several samples were thereby available which was important to improve the reliability of the performed dispersion measurements.

3.2 ENGINE RIG EXPERIMENTS

Two different engine rig experimental set-ups were used in this project. The first set-up, of more traditional type, was used for both Paper I and II and the experiments were performed at Johnson Matthey in Gothenburg.

3.2.1 SET-UP

The traditional engine rig simply consisted of an engine connected to the catalyst that was to be investigated. The exhaust properties were varied by

controlling the engine operating point and the temperature, flow rate, and composition before and after the catalyst were measured.

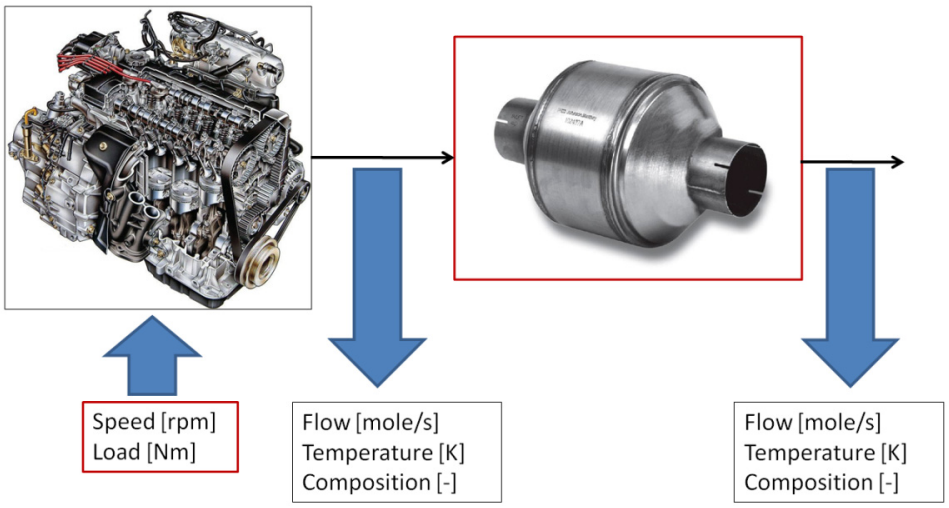

FIGURE 8 *Traditional engine rig set-up. The red frames around the catalyst and the engine operating point indicate that these are controlled by experimental design.*

A Euro IV calibrated heavy duty diesel engine with disabled exhaust gas recirculation (EGR) was used as the exhaust source and Swedish MK1 diesel, a commercial low-sulfur (less than 10 weight ppm sulfur [23]) diesel, was used as fuel. The engine was equipped with a dynamometer control system enabling independent control of load and speed.

The temperature and composition measurements were made according to figure 9 where the downstream catalyst position (Cat. 2) was left empty if only one catalyst was used.

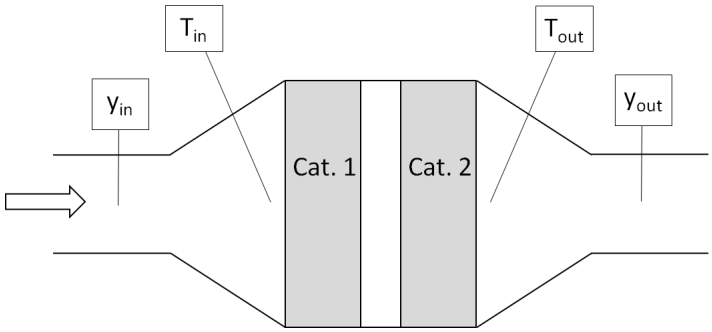

FIGURE 9 *Catalyst measurement points where T indicates temperature and y composition*

The temperatures were measured with 3 mm thermocouples positioned at the center of the pipe and close to the catalysts. The inlet gas composition was

measured just before the pipe expansion and the outlet gas composition was measured directly downstream the pipe contraction.

3.2.2 EXPERIMENTAL DESIGN

To obtain a widespread experimental range, five different catalyst configurations with different noble metal loading, lengths, and washcoat thicknesses were used. Not all the configurations in table 1 were used in all full scale studies. Configurations a to d were used in Paper I and II and configurations a, d and e were used in Paper IV.

As mentioned in the introduction the available exhaust composition, flow and temperature is limited by the operating points of the engine. It also takes several minutes for the catalyst inlet conditions to stabilize when switching between operating points, which means that experimental time was a factor when deciding the number of different operating points when the full transient behavior was of interest. An important part of the current work was to investigate what experiments were suitable for parameter estimation and therefore both transient and steady-state data was desirable. Since the number of catalyst configurations was large and some replicates also were necessary only 8 different operating points were selected according to table 3.

TABLE 3 *Engine operating points and levels of variables, Med=medium*

Number	**Description**				
	NO_x	**HC + CO**	**O_2**	**Temp.**	**Flow**
1	Low	High	High	Low	Low
2	Low	High	High	Low	Med
3	High	Med	Med	Med	Low
4	Med	Low	Med	Med	High
5	High	Low	Low	High	Med
6	Med	Low	Med	Med	High
7	High	Low	Low	High	Med
8	Med	Low	Low	High	High

The operating points were selected manually but were later confirmed to be close to a D-optimal selection (see section 2.2) with a model based design analysis of the engine map in temperature, concentrations and flow. Figure 10 shows an example of how the operating points spanned over the engine map for the case of exhaust temperature.

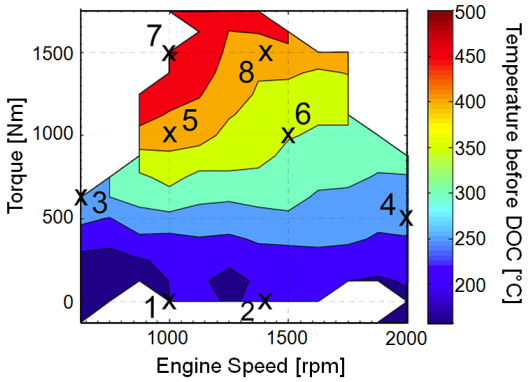

FIGURE 10 *Temperature engine map and selected operating points*

The operating points were selected to make as large steps as possible in the different variables including concentrations of NO, NO_2, HC, CO and O_2 as well as temperature and flow rate with the purpose of making the experimental space as large (and orthogonal) as possible. Some of the variables, such as concentrations of NO and NO_2 and concentrations of HC and CO, are closely correlated and it was difficult to create transients where they were changed independently. This was also the case for O_2 and temperature, i.e. an operation point with low temperature would have high oxygen concentration and an operation point with high temperature would have low oxygen concentration. This meant that some of the input variables could not be varied independently. A good experimental plan would however ensure that the variables were varied as independently as possible.

The operation points were run in the order 1, 7, 2, 8, 3, 4, 5, 6 for all catalyst configurations to make as large transient changes as possible in as many variables as possible. For some of the configurations several additional sequences were also run. To achieve steady state conditions all points were run for 15 minutes each.

3.3 SCANIA ENGINE RIG

When switching between two engine operating points it generally takes several minutes before the properties of the emissions have stabilized. The main reason is the large thermal mass between the engine and the investigated catalyst which will not only affect the transient behavior of the temperature but also of the concentrations. This not only makes the experiments time

consuming, but it also complicates the transient modeling of the DOC since the changes in inlet properties are far from ideal step functions.

Kolaczkowski et al. [24] presented a method where a pollutant was injected between the studied DOC and the engine to achieve transient data without changing the engine load point. This method also presents the great benefit that the heat accumulation problem is avoided, since the engine load and thereby the temperature is constant, and thus very fast transients in concentrations can be achieved. Sjöblom [25] further extended this concept by also having the possibility to reduce the flow (increase residence time) and control the temperature.

In the Scania engine rig (Paper IV) a set-up was presented where additional catalysts were inserted upstream the investigated catalyst. By using different bypass settings and injection of urea the catalyst inlet composition could be changed without changing the engine operating point resulting in faster transients.

3.3.1 SET-UP

In the set-up of the Scania engine rig an extra DOC with the possibility for bypass flow and an SCR with urea injection were mounted before the investigated catalyst (DOC 2), as illustrated in figure 11.

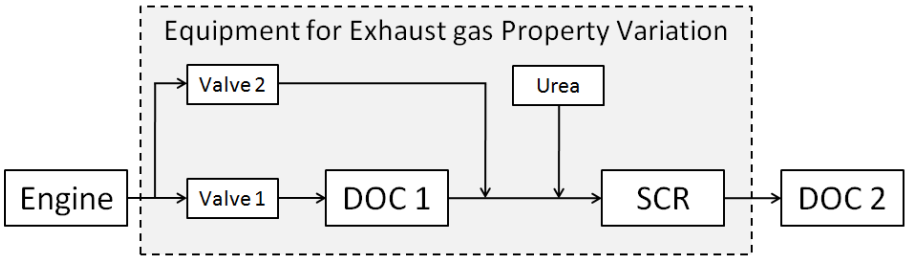

Figure 11 Experimental set-up. "DOC 2" is the test object to be studied

The fraction of exhaust gas flow through DOC 1 allows variation in the conversion of HC and CO to CO_2 and H_2O, and the conversion of NO to NO_2. By injecting different amounts of urea the conversion of NO_2 and NO to N_2 is controlled and the ratio of NO_2 to NO_x can be adjusted, the engine was also tuned to run with late fuel injection to achieve high HC and CO concentrations. A Vanadium based commercial SCR and a commercial platinum only DOC were used for exhaust gas property variation.

3.3.2 EXPERIMENTAL DESIGN

The fast transients and the wide range of possible settings for the DOC bypass and urea injection made it possible to achieve a wide variation of exhaust compositions for every engine operating point in a short time span. Instead of searching for the best points in the engine map, the focus of the experimental design was instead put on finding the operation of the DOC bypass and urea injection that would generate the data best suited for parameter estimation.

Three different experimental types with different operation of DOC bypass and urea injection were evaluated:

1. Urea injection and SCR were removed from the configuration shown in figure 11. Valve 1 was switching between 20% and 90% open at the same time as valve 2 was switching between 80% and 10% open every 20 seconds.
2. Set-up was as in figure 11. Urea was injected for 20 seconds followed by 20 seconds of no injection. Valve 1 and 2 were in locked positions.
3. Set-up was as in figure 11. Valve positions were switching every 20 seconds. Urea injection was switched on/off every 20 seconds with a 10 seconds delay relative to the valve positions switching.

All experiments were run at more than 20 different engine operating points and to further expand experimental space several catalyst configurations were also used for the same experiments.

3.4 LAB EXPERIMENTS

The purpose of the lab experiments was to provide appropriate data for developing a detailed kinetic model where the conditions for the catalyst model to separate kinetics and mass transfer were favorable. To achieve these conditions catalysts with inert washcoats were used (see section 3.1.2) and temperature ramp experiments were performed, both with individual components and on a mixture.

3.4.1 SET-UP

The inlet gas composition was controlled by mass flow controllers and the gas mixture temperature was controlled by an oven that also contained the monolith itself. The flow through the reactor was heat exchanged with the

monolith in a recirculating design according to figure 12. This design was chosen to achieve a more even temperature distribution in the monolith compared to what would be possible if the monolith would be heated only by the incoming flow.

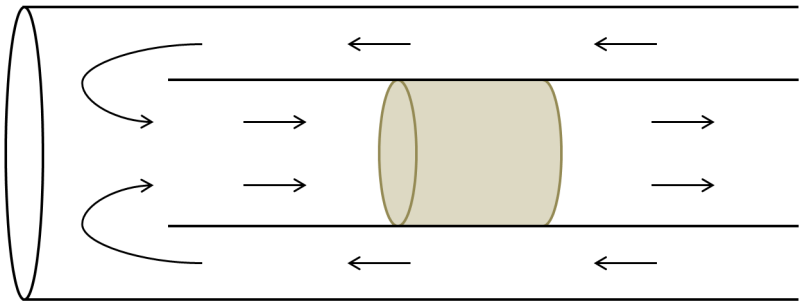

FIGURE 12 *Illustration of the lab rig heating principle. Note that the incoming flow surrounds the monolith*

Gas temperature was measured with 1.5 mm thermocouples positioned at the center of the pipe close to the catalyst outlet. The gas phase concentrations were measured after the catalyst with separate analyzer units. The concentration of CO was measured with infrared spectroscopy, NO and NO_2 were measured with chemiluminescence, total hydrocarbons were measured with flame ionization and O_2 was measured with an electrochemical cell.

The gas composition entering the catalyst was adjusted to the demanded inlet conditions at low temperature before the heating ramp was applied; the inlet concentrations in the presented results are therefore considered equal to the set-points of the gas flow controller.

3.4.2 EXPERIMENTAL DESIGN

To achieve good conditions for parameter estimation it is important to have experimental conditions that span the data range, where the model is aimed to be applied, as effectively as possible. In the lab-scale study the desired model application was simulation of full scale systems with heavy duty diesel engines which meant that the catalyst inlet temperature and concentrations should be in the range of what such an engine can produce. The experiments should include both a complete synthetic exhaust gas mixture as well as simpler ones that enable estimation of parameters where the reactions take place with or without competition between the different oxidation reactions. It was also important that conversions of the components also coved a wide span. To

achieve these desired properties of the data four different experiments were performed on every catalyst configuration. The inlet concentrations for these experiments were kept constant at the levels given in table 4 while the temperature was ramped from low to high and back to low.

TABLE 4 *Inlet concentrations for the performed experiments*

	NO [ppm]	**NO_2 [ppm]**	**C_3H_6 [ppm]**	**CO [ppm]**
CO light-off	-	-	-	100
C_3H_6 light-off	-	-	50	-
NO light-off	800	-	-	-
Full gas mix	800	80	50	100

In addition to the components in table 4 all gas mixtures also contained 5 % CO_2, 5 % H_2O, 14 % O_2 and the balance N_2. For all experiments a low initial temperature was chosen to avoid reaction at the starting point of the experiments. The maximum temperatures of the different experiments were chosen to achieve a conversion at or close to 100% for the catalysts with highest platinum loading and no inert washcoat layer (catalyst 2 in table 2).

4 MODELLING

4.1 REACTOR MODEL

A full scale catalyst monolith with varying inlet properties displays a highly dynamic behavior. This means that the catalyst outlet conditions will not only be influenced by the current inlet conditions but also those at previous time points. To describe this behavior a catalytic reactor model with accumulation terms is needed. The level of detail needed in the model is of course depending on its purpose. If all details of mass, heat and momentum transport are required and computational time is not an issue then a complete 3D CFD model (figure 13) may be the best option. In this work the model was used for parameter estimation which means that it was used in an iterative process to fit model parameters to measurement data and as such the simulation time is also a very important factor.

As described in the introduction (section 1.2.1) both the heat and the mass transfer in a monolith catalyst occur over a wide range of inter-connected length scales. For reaction to occur the reactants first need to be convectively transported from the gas phase to the solid washcoat surface. From the surface they need to further diffuse into the washcoat with pores that have pore diameters less than a micro meter to finally react on the noble metal active sites.

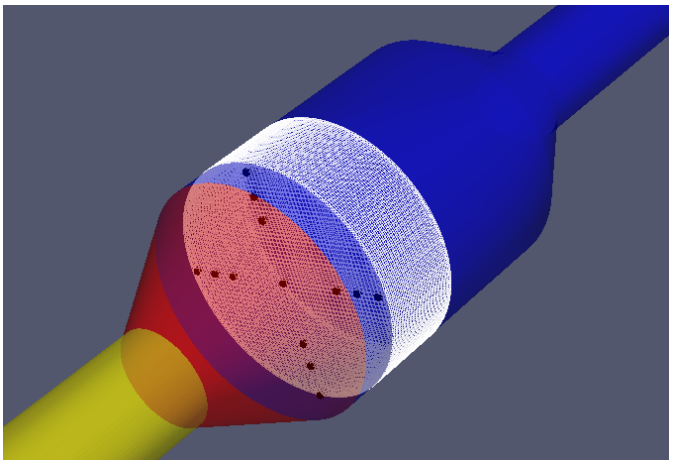

FIGURE 13 *Example of CFD model showing the computational mesh of the monolith*

A full scale catalyst of the size used in this project has over 40 000 channels. If all channels are to be modeled individually an extremely high resolution is needed if phenomena like concentration gradients in the washcoat (as a function of reaction rates and heat and mass transport), and radial temperature gradients are to be modeled. A model of such complexity is not feasible for parameter estimation and to reduce simulation time some significant simplifications are needed.

Since the catalyst is cylindrical and thereby symmetrical around the axial axis it would be possible to simplify the model by only modeling one row of channels in the radial direction. A full scale catalyst with the specifications given in section 3.1.1 has a radial distance spanning 120 catalyst channels and the computational demand would be reduced with more than 2 orders of magnitudes if an axisymmetric modeling approach is taken. The flow upstream the catalyst is however turbulent which means that a one dimensional description of the heat and mass profile will not be able to fully replicate the true conditions. A model consisting of 120 catalyst channels is still a very complex system if modeled in three dimensions. A model with good accuracy would therefore be too computationally demanding to be used for parameter estimation. The simulation time with such a model would be in the range of hours to days and not minutes to hours [26].

The two significant transport phenomena for a full scale catalyst model are heat and mass. The porous properties of both the washcoat and the substrate make it possible for mass to be transferred between the channels. The large

transport resistance of the wall compared to the open channel does however severely limit the flow between channels and in the current study it is neglected. The distance from the engine to the catalyst is long and turbulent enough to be considered well mixed and thus the composition in the inlet to all channels can be assumed to be roughly the same.

Heat transport resistance of the substrate and washcoat is not as large as the mass transport resistance which means that heat will not only be convectively transported with the flow but also conducted in the solid material both radially and axially in the monolith. There will also be heat losses to the environment both in the piping leading to the catalyst and from the catalyst itself meaning that there will be radial temperature gradients both in the catalyst inlet and inside the catalyst. The magnitude of these gradients are largely dependent on the experimental set-up where insulation and heating can be used to significantly reduce the gradients. In a method presented by Štěpánek et al. [27] a full scale CFD-based model was used to solve the 3D temperature profile in the catalyst which in turn was coupled to a simple 1D model for reactions in the catalyst washcoat. A similar approach was taken by Stamatelos et al. [28] but the solid energy balance was solved for an axisymmetric 2D model.

The most common type of model for simulation of monolith converters is however still significantly simpler 1D models for both heat and mass [29] where all channels are assumed to have the same inlet conditions, heat loss (if any), and flow rate. The advantage with these kinds of models is of course high simulation speed and the drawback is reduced accuracy [30].

In this work a 1D/2D single channel model, closely based on the model presented by Ericson et al. [31], was chosen since it was considered a good compromise between accuracy and computational speed [32]. Due to surface tension effects during the washcoating process the washcoat usually is thicker in the corners of the channel and thinnest furthest from corners. In the current work the washcoat formulation was however simplified to a slab representation with constant washcoat thickness to avoid the need of a third dimension to model the washcoat.

The gas phase in the channel was assumed to have fully developed laminar properties and thereby a discretization in the axial direction only (1D) was assumed to be sufficient when combined with a film transport model between gas bulk and washcoat surface.

The wide temperature range of vehicle exhaust together with the need to package maximum activity into a given volume of the converter for on-board space-efficiency, unavoidably leads to transport limitations. This means that large gradients in the washcoat are likely to occur which makes the washcoat discretization specifically important for a proper description of the behavior of the system. The washcoat was therefore chosen to be discretized both radially and axially (2D), see figure 14. The method used for discretization was tanks in series mainly selected for its robust properties in transient simulations.

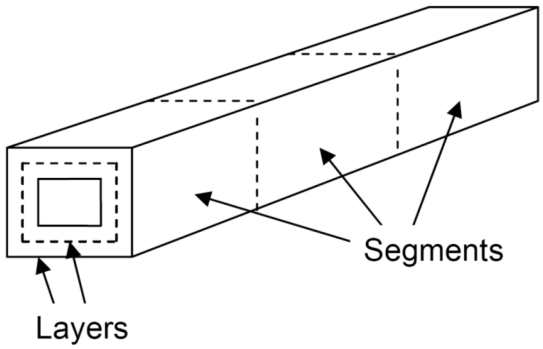

FIGURE 14 *Illustration of the catalyst discretization principle of a single channel*

As mentioned above, there are some clear differences between heat and mass transfer and the modeling of the different phenomena are described separately below. For full details see Paper I.

4.1.1 MASS TRANSPORT

For every tank and species the balance [in] – [out] ± [produced or consumed] = [accumulation] is made. In the gas bulk no reaction takes place which means that the balance only includes convective transport with the flow and transport to and from the washcoat. The diffusive transport in the gas bulk in the axial direction is not taken into account in the mass balance since it is considered negligible compared to the convective flow.

The transport resistance between the gas bulk and the first washcoat layer is modeled as two parts; firstly it is the film transport resistance and secondly it is the diffusive transport resistance of half the washcoat layer thickness. This

configuration is chosen since it will represent the concentration in the center of the washcoat layer and thus a good estimate of the average concentration in the volume represented by the tank. The first two studies (Paper I and II) used the asymptotic value for the Sherwood number [33] but for the other studies it was replaced by the model for quadratic laminar channels introduced by Hawthorn [34] (see Paper III for full equation). Entrance effects were neglected for all studies.

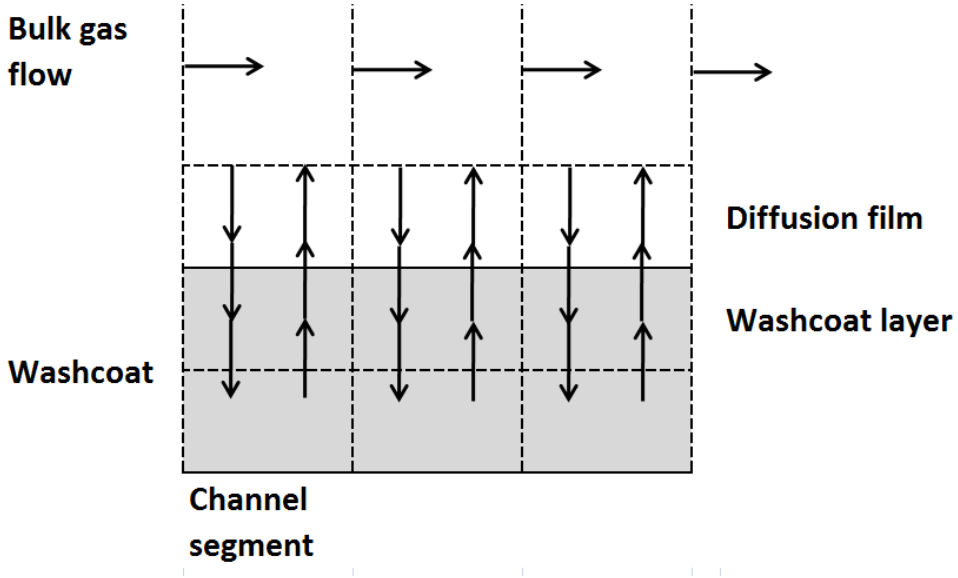

FIGURE 15 *Mass transport discretization*

For further transport in the washcoat the resistance also consists of two parts which are the diffusive resistances of half the washcoat thickness of both layers. The axial transport in the washcoat is neglected since the axial transport distance is about 3 orders of magnitude larger than the radial transport distance. A description of the mass transport in the washcoat and its discretization is shown in figure 15.

The model will have a very dynamic behavior which means that accumulation terms are needed for an accurate description. Accumulation terms do however generate a significant increase in the computational cost and if the transient time scales are small the model stiffness and instability may increase. Accumulation terms should therefore be carefully analyzed before inclusion in the model. In the case of gas phase concentration, the characteristic time constants are small which means that a new steady state point will be reached

within tenths of a second if the inlet concentrations are changed at constant temperature (see section 6.2 for example). The characteristic time constant for temperature is, on the other hand, large and will dominate the dynamic behavior of the gas phase concentrations and as a result accumulation of gas phase species both in the gas bulk and in the washcoat were neglected. In detailed kinetic models the adsorbed species influence all reaction rates and are also important accumulation terms necessary to describe certain transient phenomena such as hysteresis.

Since two different kinetic models were used in this dissertation, one global and one detailed, there is also two ways of describing the influence from adsorbed species. In the global kinetic model used in the first two studies the adsorbed species dependence is modeled by an inhibition term only as a function of temperature and the washcoat concentrations. The transient behavior of the adsorbed species is thereby not described by an accumulation term (the inhibition term is independent of previous temperature and concentrations) which will make this kinetic model less computationally demanding but also less suitable to describe transient behavior. The global kinetic model was applied to data where temperature, flow and species concentration could not be changed independently which made effects of adsorbed species accumulation difficult to identify. The detailed kinetic model derived from lab data used accumulation of adsorbed species which was necessary to model the hysteresis in the experiments. This made the model slower and less stable than the global one but also more accurate.

4.1.2 HEAT TRANSPORT

The modeling of the heat transport in the gas bulk is analogous to the mass transport in the gas bulk; the discretization is only made axially, the thermal conduction is neglected, and the film resistance is calculated from correlations. The first two studies used the asymptotic value for the Nusselt number [33] but for the other studies it was replaced by the model for quadratic laminar channels introduced by Hawthorn [34] (see Paper III for full equation). The modeling of the heat transport in the washcoat on the other hand displays several differences from how the mass transport was modeled.

The main difference between modeling of mass and heat transport originates from the fact that the heat transport resistance is much lower (high heat conduction) than the mass transport resistance (low effective diffusivity). For the mass transfer modeling the long axial transport distance coupled with the high transport resistance meant that axial mass transport in the washcoat was neglected. In the case for heat transport the long axial distance is counterbalanced by the low transport resistance which means that axial heat transport cannot be neglected. The efficient heat transport in the washcoat also means that transport in the significantly shorter radial direction will be very efficient and as a result the radial heat transport resistance was neglected. Neglecting the radial heat transfer resistance means that the radial discretization of the washcoat that was necessary for mass transfer can be simplified to a single layer for heat transport. An illustration of the discretization can be seen in figure 16.

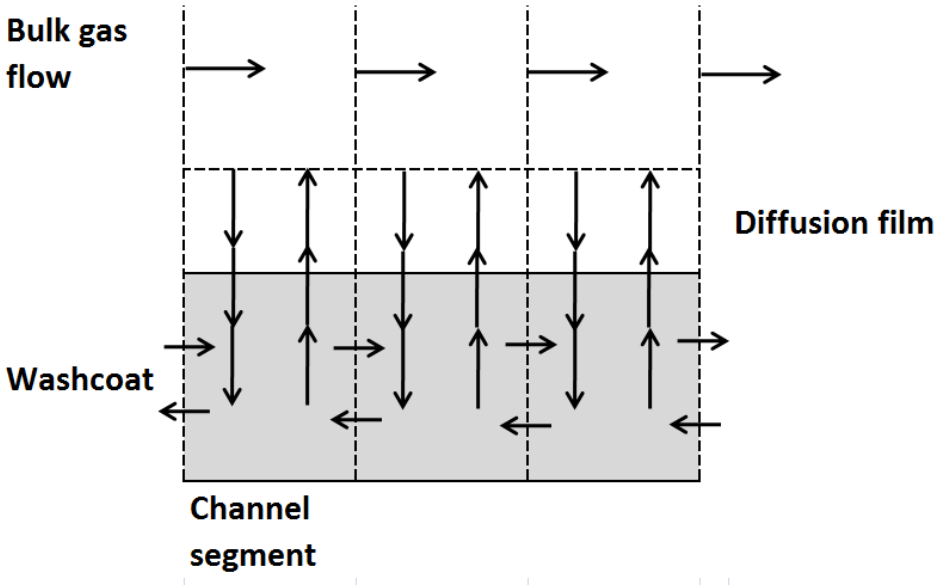

FIGURE 16 *Heat transport discretization*

The efficient heat conduction in the washcoat and substrate means that phenomena like heat loss to the environment and heat accumulated in surrounding materials such as insulation and canning will have a large influence on the behavior of the monolith if adiabatic conditions do not prevail. Since only one channel is modeled, a heat loss term and extra heat accumulation term is added to every washcoat channel segment to model the two aforementioned phenomena (at lab-scale these terms were however

neglected). Modeling the heat loss to the environment as equal for all channels is a rough simplification but the alternative of modeling more channels with different temperatures and heat losses was considered to require a too large increase in computational demand.

4.1.3 DISCRETIZATION

The number of segments and layers are of utmost importance for the performance of the model. A too low number of segments and layers will make the simulation dependent on the discretization and a too high number of segments and layers will lead to unnecessarily long simulation times. For the parameter estimation performed in this project a model discretized as 10 (axial) segments and 8 (radial) layers was considered a good tradeoff between model accuracy and simulation time. It should be noted that the number of axial segments is lower than what is theoretically necessary to model a tube reactor [35] which will result in an over representation of axial dispersion.

A major influence on the model performance is not only the number of segments and layers but also how they are distributed. In general the faster a property changes in one direction a finer discretization is needed to fully resolve a concentration or temperature gradient. For a catalyst at high temperature, the reaction rate will be high which means that some components may be consumed before they have diffused radially through the washcoat. Also, the fact that diffusive flux of all components is set to zero at the washcoat-carrier material interface means that concentration gradients will approach zero close to the carrier material and be steeper at radial positions close to the surface. In other words a fine discretization close to the washcoat surface would be needed but not close to the carrier material. At low temperatures the reaction rate will be slow and concentration will not change much with radial position and thus there is little need for a fine radial discretization. With this in mind, a washcoat discretization that decreased linearly with radial position was chosen which is demonstrated for eight layers in figure 17.

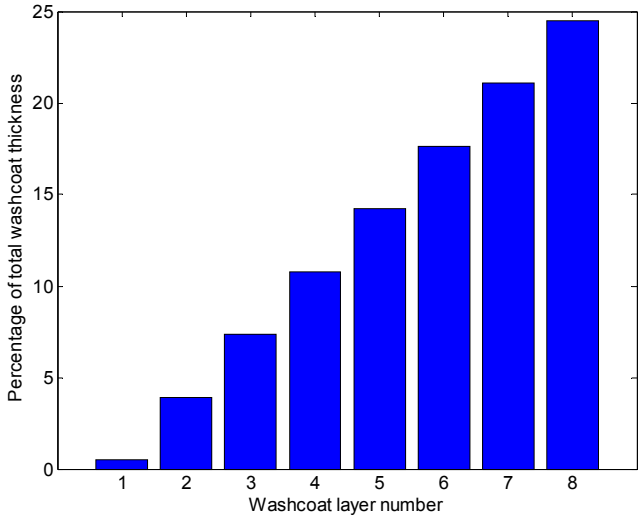

FIGURE 17 *Radial washcoat discretization for eight layers*

For axial discretization the same reasoning can be applied as for radial discretization; it is more likely that the axial gradients are larger close to the inlet than close to the outlet. This indicates that a discretization decreasing with axial position would be preferable also in this direction. However, a conversion close to 100 % - which would be the case for a steep concentration gradient close to the inlet is not generally desired since these kinds of experiments are less informative in a kinetic parameter estimation point of view. The dynamic behavior of the model also means that different parts may experience large gradients at different conditions. For example when the inlet temp is changing from high to low the outlet end of the monolith can have a higher temperature than the inlet end and as a result gradients can be steeper near the outlet. With this in mind an equidistant axial discretization was selected.

4.2 KINETIC MODELS

Large efforts have been made to construct kinetic models for the DOC both of global type [15, 36-38] and microkinetic type [39-41]. The microkinetic models describe all reactions divided into elementary steps, which makes it possible to derive estimated kinetic parameters from reaction rate theory. In the global models the elementary steps are assumed to be either rate-determining or in equilibrium, which makes it possible to derive rate expressions for the overall reactions with a significantly reduced number of parameters compared to the

microkinetic models [10]. These global rate expressions generally use only gas phase concentrations which are also used to account for inhibition, adsorption and desorption. This means that the accumulation of adsorbed species is neglected which is less of a concern for species with very low surface coverages but for others it is clearly detrimental for accurate predictions of transients.

Since catalytic reaction mechanisms are often not understood down to the elementary step level the global rate expressions are rarely strictly derived from elementary reaction steps. Instead, they are often adjusted and sometimes expanded with additional semi-empirical expressions to better describe observed experimental data. In addition, reaction steps may be neglected and parameter values lumped all with the aim of reducing the kinetic model complexity and number of adjustable kinetic parameters. These kinds of simplifications and modifications of rate expressions may also lead to the kinetic parameters having less of a physical nature and more importantly becoming more case-specific and less generally applicable [10]. Nevertheless, the far lower computational demands of global kinetic type models means that they are often the model-type of choice for aftertreatment design evaluations and control algorithms. It should be noted that exclusion of adsorbed species in the global models will make them less suitable to describe transient behavior even though it may not be an issue for species with low surface coverage.

The simplest versions of the DOC kinetic models only describe the oxidation reactions of CO, HC, and NO. In addition HC is often represented as one molecular species, usually propene [15, 42, 43]. The exhaust composition is far more complex than just one type of hydrocarbon species and there are examples of kinetic models [28, 36] that have been expanded with several types of HC. Other additional reactions that may be added include H_2 oxidation [28, 41] and HC reduction of NO_x [37, 44] or by NO_2 [36]. In this work both a global kinetic model, with only three reactions, and a detailed kinetic model, with twelve reactions, have been used in the different studies. The detailed kinetic model is not microkinetic model with the definition given above but contrary to the global kinetic model, surface species are modeled and included in the reaction rates.

4.2.1 GLOBAL KINETIC MODEL

The focus of the first two studies was developing the parameter estimation method rather than on the required model formulation or level of detail of the kinetic model. The kinetic model used in these studies was of Langmuir-Hinshelwood type and was originally suggested in the classical work by Voltz et al [15] and later modified by Oh and Cavendish [42]. This model, which has been widely and frequently used in DOC modeling over the years, only includes three reactions of which one is an equilibrium reaction:

$$CO + \frac{1}{2}O_2 \rightarrow CO_2$$

$$C_3H_6 + \frac{9}{2}O_2 \rightarrow 3\ CO_2 + 3\ H_2O$$

$$NO + \frac{1}{2}O_2 \rightleftharpoons 2\ NO_2$$

The reaction rates were calculated according to equations 2 to 6.

$$r_1 = \frac{k_1 y_{CO} y_{O_2}}{G(y_i, T_s)} \tag{2}$$

$$r_2 = \frac{k_2 y_{C_3H_6} y_{O_2}}{G(y_i, T_s)} \tag{3}$$

$$r_3 = \frac{k_3 y_{NO} y_{O_2}}{G(y_i, T_s)} \left(1 - \frac{K'}{K_p}\right) \tag{4}$$

$$K' = \frac{y_{NO_2}}{y_{NO} y_{O_2}^{\frac{1}{2}}} \tag{5}$$

$$G(y_i, T_s) = T_s\left(1 + K_4 y_{CO} + K_5 y_{C_3H_6}\right)^2 \left(1 + K_6 y_{CO}^2 y_{C_3H_6}^2\right)\left(1 + K_7 y_{NO}^{0.7}\right) \tag{6}$$

where K_j is the reaction rate coefficient for the inhibition terms in the denominator G and K_p is the equilibrium constant for NO oxidation. At thermodynamic equilibrium, K_p will be equal to K' and reaction rate r_3 will be equal to zero. Both reaction rate coefficients k_j and K_j were described by Arrhenius expressions:

$$k_j = A_j \exp\left(-\frac{E_{A,j}}{RT_s}\right) \tag{7}$$

The start values for estimation of kinetic parameters were taken from Wang et al. [43] where results from several studies [45-51] were compiled. The initial values for kinetic parameter estimation used in this study are shown in table 5.

TABLE 5 *Start values for kinetic parameters estimation*

Index	**Pre-exponential factor [mole K/(m²s)]**	**Activation energy [kJ/mole]**
j	A	Ea
1	1.00×10^{17}	80.0
2	4.00×10^{20}	100.0
3	4.50×10^{14}	70.0

Index	**Effective entropy of adsorption*** **[-]**	**Heat of adsorption [kJ/mole]***
j	A	Ea
4	65.5	-8.0
5	2080	-3.0
6	3.98	-96.5
7	479000	31.0

*For simplicity these parameters will be referred to as pre-exponential factors and activation energies in upcoming discussions even though they have a different physical meaning

The kinetic parameters in equations 2 to 6 are highly correlated and since the parameter values in table 5 were taken from different studies, the fit of the model to experimental data was expected to be poor before any parameter tuning was performed. However, the parameters were successfully used as a starting point for parameter tuning of a DOC against engine rig data by Wang et al. [43] which was also the intended application in the present work.

4.2.2 DETAILED KINETIC MODEL

The structure of the detailed kinetic model was derived by analyzing the experimental data and the parameter values were a result of parameter estimation. The parameter values will be presented in Results and Discussion but the structure will be presented here even though it also was a result of the study performed (Paper III). The final structure of the detailed kinetic model is given in table 6.

TABLE 6 *Final structure of the detailed kinetic model*

#	Reaction	Rate
1	$O_2(g) + 2* \rightarrow 2O*$	$r_1 = c_{O_2}\theta_v^2 k_1$
2	$2O* \rightarrow O_2(g) + 2*$	$r_2 = \theta_O^2 k_2$
3	$NO_2(g) + * \rightarrow NO_2*$	$r_3 = c_{NO_2}\theta_v k_3$
4	$NO_2* \rightarrow NO_2(g) + *$	$r_4 = \theta_{NO_2} k_4$
5	$NO(g) + O* \rightarrow NO_2*$	$r_5 = c_{NO}\theta_O k_5$
6	$NO_2* \rightarrow NO(g) + O*$	$r_6 = \theta_{NO_2} k_6$
7	$CO(g) + * \rightarrow CO*$	$r_7 = c_{CO}\theta_v k_7$
8	$CO* \rightarrow * + CO(g)$	$r_8 = \theta_{CO} k_8$
9	$CO* + O* \rightarrow CO_2(g) + 2*$	$r_9 = \theta_{CO}\theta_O k_9$
10	$CO* + NO_2* \rightarrow NO(g) + CO_2(g) + *$	$r_{10} = \theta_{CO}\theta_{NO_2} k_{10}$
11	$C_3H_6(g) + 9O* \rightarrow 3CO_2(g) + 3H_2O(g) + 9*$	$r_{11} = c_{C_3H_6}\theta_O k_{11}$
12	$C_3H_6(g) + 9\,NO_2* \rightarrow 9NO(g) + 3CO_2(g) + 3H_2O(g) + 9*$	$r_{12} = c_{C_3H_6}\theta_{NO_2} k_{12}$

Reaction number 1-8 can be described as equilibrium reactions where even reaction numbers are desorption and uneven reaction numbers are adsorption while reaction 9-12 are oxidation reactions. The starting point in the development of the kinetic model was reaction 1-6 that represented a simplified version of the detailed kinetic model presented by Olsson et al. [52]. The simplification made was that surface NO was neglected based on the fact that no clear hysteresis for NO was found in the experimental data. A clear hysteresis was on the other hand found in the dedicated CO oxidation experiments which is exemplified in figure 18. The hysteresis is a result of competitive adsorption of CO and O where CO will dominate the surface coverage at the start of the experiment, thereby delaying the light-off. To capture this behavior CO was needed to be included in the model as a surface species which introduced reaction 7-9 in the model.

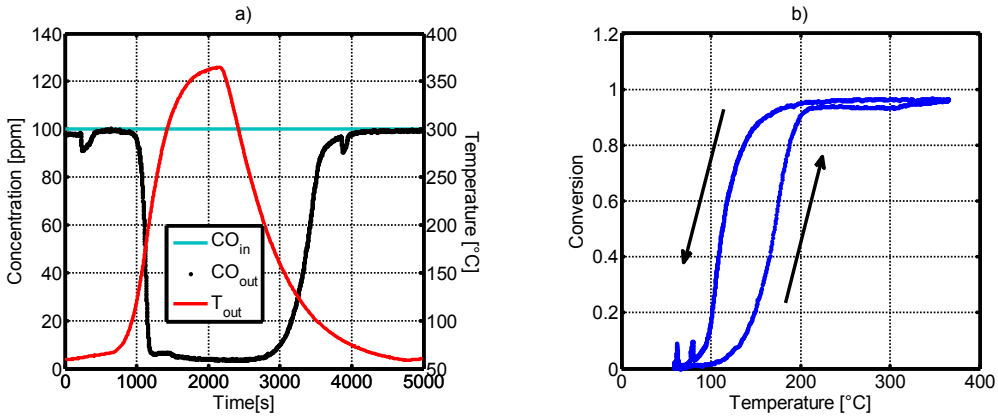

FIGURE 18 *Hysteresis for CO oxidation in lab-scale experiments*

In the experiments with a more complex gas mixture (full gas mix in table 4) a reduction of NO_2 to NO was measured at low temperatures at the same time as CO was oxidized, see figure 19. The NO oxidation reaction would at these conditions react towards a thermodynamic equilibrium with less NO and more NO_2 and the reaction mechanism must thereby be more complex than the first nine reactions in table 6. Reaction 10 was therefore included in the kinetic model to describe reaction between adsorbed CO and adsorbed NO_2.

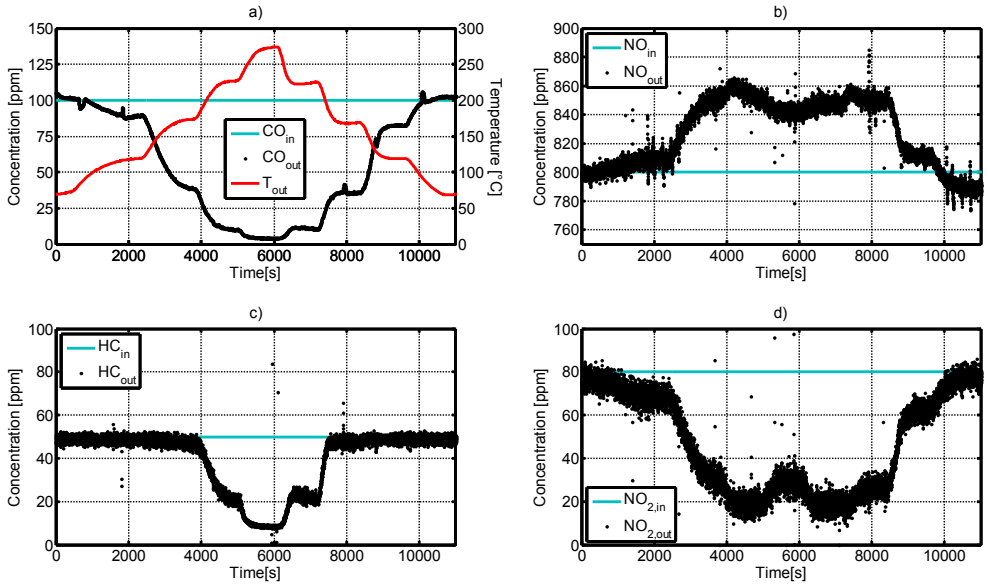

FIGURE 19 *Full gas mix experiment for catalyst 4*

The hysteresis for propene was deemed not prominent enough to warrant an inclusion of propene as a surface species in the model. As a result, propene oxidation was modeled as a reaction between adsorbed O and gas phase propene. From the gas mix experiments it is difficult to conclude if propene is

oxidized by O_2 and NO_2 or by O_2 alone. The fact that oxidation by NO_2 was observed at similar conditions [53] and that NO_2 showed strong oxidizing properties for CO was, however, strong enough arguments for including the reaction in the kinetic model.

All reaction rate coefficients, k_j, were described by Arrhenius expressions according to equation 7. The reaction rate description for reaction 7 also includes a temperature dependent pre-exponential giving that rate expression an additional factor of $T^{0.5}$. The reaction rates are all in the unit of mole/(s ×kgPt).

5 PARAMETER ESTIMATION

With the experimental plan carried out and the catalyst and kinetic models selected the parameter estimation can finally be performed. The standard procedure of parameter estimation for automotive catalysts is to use all experimental data points to estimate kinetic parameters only. In the current project the estimation of kinetic parameters were complemented by estimation of heat and mass transport parameters to better describe the dynamic behavior of the catalyst. A method improving the final fit by performing parameter estimation on sub-sets of the data selected by Multivariate Data Analysis (MVDA) was also evaluated (Paper II).

5.1 ADJUSTABLE PARAMETERS

At lab-scale the heat losses to the environment can usually be kept at negligible levels (insulation or heating of the monolith are two common measures) and also the mass transport resistance can be reduced by using thin washcoat layers or even using powder of a crushed monolith [54]. In the case of full scale catalysts heat- and mass transfer limitations are more likely to have an important influence on the results, as has been discussed above. The parameters affecting the heat- and mass transfer resistance are difficult to measure and the best option may be to instead use simplified models where a few parameters are tuned to experimental data.

The parameter estimation is performed with parameters in scaled and centered forms [55]. Which means that the estimated parameter is equal to an original value from literature or previous estimation plus/minus the adjustable

parameter, p, times a weight factor, w. For example the activation energy is estimated by

$$E_{A,j} = E_{A,j}{}^{o} + w_{Ea,j}p_{Ea,j} \quad (8)$$

where the superscript "o" indicates that this is the original value. The value of the weight factor is selected to make the parameter sensitivity more balanced.

5.1.1 KINETIC PARAMETERS

When tuning kinetic parameters it is important to be well aware of the properties of the chosen kinetic model. The global kinetic model is generally more robust in its construction and may for example contain factors to ensure that thermodynamic restriction are always fulfilled; for detailed kinetic models this is however not likely to be the case.

If the model contains both the forward and backward reaction in an equilibrium reaction it would not be a good choice to tune the parameters of both reactions since this would lead to very high correlation. For the detailed kinetic model this means that several of the kinetic parameters presented in table 6 should not be tuned if computational efficiency is important. The choice was therefore made to mainly estimate the desorption reactions while the adsorption reactions were kept constant. The global kinetic model does contain one equilibrium reaction in the NO oxidation reaction but in effect this reaction only goes in one direction with a driving-force factor that approaches zero as thermodynamic equilibrium is approached. All the pre-exponential factors and activation energies for the global kinetic model were therefore tuned to experimental data.

For reactions governed by thermodynamic limitations, such as the NO oxidation, it is also important that the thermodynamic limitations are not violated when the kinetic parameters are estimated. For reasons previously stated this is not an issue for the global kinetic model but for the detailed model additional restriction need to be applied. The parameters A_6 and $E_{A,6}$ (table 6) were not directly tuned but were continuously updated to maintain the thermodynamic limitations of the NO oxidation reaction according to equations 9 and 10.

$$E_{A,6} = \frac{1}{2}\left(E_{A,1} - E_{A,2}\right) + \left(E_{A,4} - E_{A,3}\right) + \left(E_{A,6} - \Delta H_{net}\right) \quad (9)$$

$$A_6 = \left(\frac{A_1}{A_2}\frac{P}{RT_{ref}}\right)^{\frac{1}{2}}\frac{A_4}{A_3}A_5 \exp\left(\frac{-\Delta S_{net}}{R}\right) \quad (10)$$

where equation 9 maintains the overall enthalpy change of NO oxidation and equation 10 maintains the overall entropy change.

The parameter estimation of activation energies is a linear amplification of the original activation energies as already shown in equation 8. The parameter estimation of pre-exponential factors is performed in three steps [56]. As a first step the reaction rate coefficients are centered on a reference temperature with the purpose of reducing the correlation between activation energies and pre-exponential factors.

$$k_{ref,j}{}^{o} = A_j{}^{o} \exp\left(-\frac{E_{A,j}{}^{o}}{RT_{ref}}\right) \quad (11)$$

The reaction rate coefficient $k_{ref,j}$ is scaled according to equation 12.

$$\ln\left(k_{ref,j}\right) = \ln\left(k_{ref,j}{}^{o}\right) + w_{A,j}p_{A,j} \quad (12)$$

The tuned rate constant at a reference temperature is then used to calculate the pre-exponential factor

$$A_j = k_{ref,j} \exp\left(\frac{E_{A,j}}{RT_{ref}}\right) \quad (13)$$

When equation 13 is inserted into the expression for the reaction rate coefficient in equation 7, the following expression for the tuned reaction rate coefficient is obtained

$$k_j = k_{ref,j} \exp\left(-\frac{E_{A,j}}{R}\left(\frac{1}{T_s} - \frac{1}{T_{ref}}\right)\right) \quad (14)$$

This transformed expression of the reaction rates will reduce the temperature dependence of the pre-exponential factor and increase the temperature dependence of the activation energy, thus reducing parameter correlation. The method was first introduced by Hawthorn et al. [34].

It has been shown that the catalyst active surface area could be used as a single parameter in a global model [57]. In addition to the pre-exponential

factors and the activation energies, an activity scaling factor was therefore also evaluated as an adjustable parameter in the first two studies as a compliment to the global kinetic model. The activity scaling factor was simply a scale factor for all reaction rates on a certain site on a certain catalyst (parameters were tuned to several different catalyst samples simultaneously). This means that the catalyst active surface area was tuned for each catalyst sample since only one single site was used in the kinetic model.

5.1.2 HEAT TRANSPORT PARAMETERS

The heat loss term and extra heat accumulation term that was added to every washcoat channel segment in the full scale models (see section 4.1.2) represent two parameters that are difficult to measure. Instead these parameters were fitted to measurement data together with a superficial environmental temperature.

The temperature in the catalyst has a very large influence on the reaction rates and conversion of the different components. For a full scale DOC in an engine rig the influence on the temperature from the reaction rate will be of less significance mainly since the concentrations of reacting species is low. To be able to perform a good parameter estimation of kinetic and mass transport parameters it is therefore important to have good accuracy in the heat transfer model but not necessarily the other way around. With this in mind the heat transport parameters were estimated before the other parameters which meant that original parameter values were used for kinetic- and mass transport parameters. By estimating the heat transport parameters separately the high correlation between reaction rates and heat transport parameters is reduced. When the heat loss parameters are estimated it will be against the residual of outlet temperature alone and when kinetic- and mass transport parameters are estimated it will only be against concentration residuals. The risk that heat transport parameters are estimated to improve the fit of outlet concentrations is thereby avoided. It should again be noted that the catalyst model used to perform parameter estimation against lab-scale data did not include a heat loss model and no such parameters were thereby tuned.

5.1.3 MASS TRANSPORT PARAMETERS

In a system where both mass transport rate limited and reaction rate limited conditions will prevail the transport in the washcoat will be of great importance for the behavior of the catalyst system as a whole. The transport resistance in the washcoat is influenced by the diffusivity at different length scales and the structure of the washcoat. Several different correlations are available to determine the diffusivities but the influence of the washcoat structure is more complicated to identify. In this study the transport resistance in the washcoat has therefore been tuned with the aim of reducing the correlation between mass transport and kinetic parameters. The method used is presented below.

The species used in the kinetic model are O_2, NO, NO_2, CO, and HC (only propene at lab-scale) which means that these also are the species whose mass transport is significant for the behavior of the model. In the catalyst model presented in [58], on which the current catalyst model is based, an expression for the effective diffusivity was derived according to equation 15.

$$D_{eff,i,k} = \frac{f_D}{\frac{1}{D_{i,k}} + \frac{1}{DK_{i,k}}} \tag{15}$$

Where f_D is a factor that takes into consideration the porosity and the tortuosity of the porous material, $DK_{i,k}$ is the Knudsen diffusivity, and $D_{i,k}$ is the gas diffusivity.

This expression describes the transport resistance in the catalyst washcoat but provides only a rough estimate. Firstly the f_D factor itself should account for both the tortuosity and the porosity of the washcoat by just one constant which makes it difficult to estimate. Secondly the structure of the pores may contain cracks and other discrepancies which would make the resistances in parallel suggested by the model (denominator of $1/D_{i,k}+1/DK_{i,k}$ in equation 15) far from reality.

The mass transport was tuned by adjusting a scaling factor for the effective diffusivities for the species taking part in the reactions.

$$f_{D_{scale},i} = f_{D_{scale},i}{}^{o} + w_{D_{scale},i} p_{D_{scale},i} \tag{16}$$

This will change the expression for the effective diffusivity according to

$$D_{eff,i,k} = \frac{f_D}{\frac{1}{D_{i,k}} + \frac{1}{D_{K,i,k}}} f_{D_{scale},i} \quad (17)$$

The value for $f_{Dscale,i}^{o}$ is typically around 1.

The species were divided into two groups, where the first group contained O_2, NO, NO_2, and CO and the second group contained HC. In the first group all species are well defined with similar diffusivities and could be expected to have similar mass transport properties in the washcoat with presumably the same bias from their true values. To reduce the number of parameters to tune, the same scale factor was used for all species in this group. The second group contained HC which was represented as C_3H_6 but in the case of real engine exhaust is a wide range of hydrocarbons with different mass transport properties. The scale factor for the second group was in other words expected to be influenced both by the hydrocarbon composition and the washcoat structure while the scale factor for the first group mainly accounted for only washcoat structure.

5.2 STANDARD METHOD OF PARAMETER ESTIMATION

The most common way to perform parameter estimation is probably to use all time points in the data to which the model is to be fitted and applying a gradient search method algorithm. This method was used in Paper I as a reference to compare to the results from Paper II where parameter estimation with PCA and D-optimal Design was used together with the gradient search method.

5.2.1 GRADIENT SEARCH METHOD

The gradient search method is very efficient for linear systems but can also be applied for non-linear systems such as catalyst models. For a non-linear system the residual function is first linearized for all parameters by the use of finite differences. The resulting matrix is an approximation of the so called Jacobian matrix that is commonly denoted as only the Jacobian (J). The Jacobian is defined according to equation 18

$$J(x,p) = \frac{df(x,p)}{dp} \tag{18}$$

where x is the variables, p is the parameter values and f is the residual. The approximation of the Jacobian is then evaluated to determine a step in the parameter space in the direction of the steepest descent. This process is repeated until the change in residual is below a certain tolerance or until a set value of steps in parameter space has been performed. The method is thoroughly described in, for example [17], but a short description of how the step in parameter space is calculated will also be given here.

The function to be minimized is the residual sum of squares according to

$$\min_p f(x,p)^2 = (y_{observed} - y_{model}(x,p))^2 \tag{19}$$

where y is the measured and simulated responses. If a specific set of data is considered the variable dependence can be dropped and equation 19 can be rewritten according to

$$\min_p S(p) = \|y_{observed} - \eta(p)\|^2 = \|z(p)\|^2 \tag{20}$$

To calculate the size of a step taken in parameter space the objective function, S(p), is first approximated by a Taylor expansion:

$$\begin{aligned} S(p) \approx S(p^0) + \left.\frac{\partial S(p)}{\partial p}\right|_{p^0} (p - p^0) \\ + (p - p^0)^T \frac{1}{2} \left.\frac{\partial^2 S(p)}{\partial p \, \partial p^T}\right|_{p^0} (p - p^0) = \\ = \left\{ \begin{array}{l} \omega = \left.\frac{\partial S(p)}{\partial p}\right|_{p^0} \\ \Omega = \left.\frac{\partial^2 S(p)}{\partial p \partial p^T}\right|_{\beta^0} \\ \delta = p - p^0 \end{array} \right\} = S(p^0) + \omega\delta + \delta^T \frac{1}{2} \Omega\delta \end{aligned} \tag{21}$$

The approximation of S(p) described in equation 21 will have a minima when the gradient is zero:

$$\omega + \Omega\delta = 0 \tag{22}$$

which gives the parameter step size according to $\delta = \Omega^{-1}\omega$. For the function $S(p)=(y-\eta)^T(y-\eta)$ the gradient ω and Hessian Ω is given by

$$\omega = -2J^T z$$
$$\Omega = 2J^T J - 2\frac{\partial J}{\partial p} z \tag{23}$$

When setting the second term of the Hessian to zero the Gauss-Newton method is obtained, where the parameter step size only depend on the Jacobian J and residual z.

It is worth noting that the linearization of the system is the most time consuming part of the gradient search method. The effect of small steps in all directions (parameter values) must be calculated by the catalyst model for all time points before a step in the steepest decent can be made. For every step made, the catalyst model will in other words be called n_p+1 times where n_p is the number of parameters that are to be estimated.

The gradient search method in this work was the trust-region-reflective method [59]. This is the standard method for over-determined non-linear least square problems in Matlab, the software used in this project. This method is implemented in the Matlab function lsqnonlin.

5.3 DEFINITION OF THE RESIDUAL

When parameter estimation is performed according to the gradient search method the target function is to minimize the residual sum of squares. The definition of the residual is therefore very important for the performance of the parameter estimation algorithm. In the case of kinetic- and mass transport parameters the residuals will be calculated from the concentrations in the outlet. How the concentrations are best used in the calculation is not trivial and several definitions of the residual have been evaluated in the current study.

Both mole fractions and temperature have been used in the residual calculations in the different studies but since temperature parameters were tuned only once, and then as the only residual, this chapter will focus on the mole fractions.

The modeled outlet flow will contain a number of different components but it may be more or less suitable to select them in the definition of the residual. The selected components should give enough information to describe the influence of the modeled reactions on the outlet concentrations but redundancy should also be avoided. For example if CO oxidation by O_2 is the only reaction, only one of the components taking part in the reaction should be used in the residual calculation since only the conversion of one component is necessary to calculate the others. In all the studies in this dissertation only NO, CO and HC were therefore necessary for residual calculation. This was based on two assumptions; firstly that NO_x reduction could be neglected and secondly that O_2, NO, NO_2, CO, and HC were the only reacting components.

5.3.1 CONCENTRATION RESIDUAL

The most straight forward formulation of the residual would be to define it as the difference between simulated outlet concentration and measured outlet concentration. If the same absolute fit to measurement data would be desirable for all components this would be a useful definition. If the concentration levels differ a lot between components a similar relative fit would probably be of higher prioritization. For the current work the NO concentrations can be about one order of magnitude higher than the concentrations of CO and HC which means that the same absolute fit for NO and CO and HC is not desirable.

To get a residual that had a more relative than absolute character a weighting method was applied in Paper I. The basis of the method was that the difference between modeled and measured outlet concentration was calculated in the selected points and then weighted depending on the component. The weighting was calculated as the inverse of the average outlet molar fraction over the entire data series. The residual was then given according to equation 24.

$$\mathrm{res_i} = \frac{\hat{y}_{\mathrm{i,out}} - y_{\mathrm{i,out}}}{\bar{y}_{\mathrm{i,out}}} \tag{24}$$

where $\hat{y}_{\mathrm{i,out}}$ is the modeled outlet mole fraction of component i, $y_{\mathrm{i,out}}$ is the measured outlet mole fraction and $\bar{y}_{\mathrm{i,out}}$ is the average outlet mole fraction. The weighting method also meant that the residual increased if the number of

points where the conversion was 100% was high, which was the case for HC and CO in the first two studies.

5.3.2 CONVERSION RESIDUAL

In Paper II an algorithm that continuously changed the selected data points used for parameter estimation was introduced which is further described in section 5.4. The point selection made the weighting against inverse of the average outlet molar fraction over the entire data series less suitable. The reason for this was that both HC and CO had a conversion at 100% for a majority of the data set giving the residuals for these components a high weight. With the new algorithm the points selected for parameter estimation were generally not the ones with 100% conversion giving a large difference between the average outlet mole fractions in the selected data points and in the entire data set. The residuals for HC and CO would therefore dominate the residual sum of squares since NO had considerably fewer data points with 100% conversion, due to thermodynamic limitations.

To decrease the difference between the components and to make the residual definition more adaptable to a changing selection of data points a different residual definition was introduced. With this definition the modeled conversion was compared to the simulated conversion limiting the residual to a value between -1 and 1 for every data point. The residual equation is given by equation 25 where considerations were also taken to the fact that the NO conversion can be limited by thermodynamic constraints.

$$\mathrm{res_i} = \left(-\frac{\hat{y}_{\mathrm{i,out}} - y_{\mathrm{i,out}}}{y_{\mathrm{i,in}} - y_{\mathrm{i,in,lim}}} \right) \frac{1}{\sqrt{n_i}} \tag{25}$$

In equation 25 n_i is the number of data points used for component i and $y_{i,in,lim}$ is the mole fraction of component i at the thermodynamic limit at inlet conditions (0 for HC and CO). The number of points selected for residual calculation may differ between the components and the $n_i^{-0.5}$ factor is included to give components with few points increased weight. For a complete derivation of the equation see Paper II.

5.3.3 CONVERSION RESIDUAL WEIGHTED BY AVERAGE CONVERSION

The conversion residual described above worked well for the engine rig data with MVDA point selection where points with varying conversion was

selected for residual calculation for all components. In the lab-scale data (Paper III) the temperatures for most experiments were lower than in the engine rig and the MVDA method was not applied. The data for parameter estimation therefore contained a majority of points where the NO conversion was close to zero which was not the case for CO and HC. Relatively low residuals for NO could therefore be achieved by just setting the reaction rates to zero. To increase the NO residuals equation 25 was expanded with an extra weight according to equation 26

$$\mathrm{res_i} = \left(-\frac{\hat{y}_{\mathrm{i,out}} - y_{\mathrm{i,out}}}{y_{\mathrm{i,in}} - y_{\mathrm{i,in,lim}}} \right) \frac{1}{X_i \sqrt{n_i}} \tag{26}$$

where X_i is the mean absolute conversion in the n_i data points for component i. The increased NO residual was mainly motivated by the objective of improving the kinetic modeling of NO_2 as an oxidizing agent.

5.4 PARAMETER ESTIMATION AIDED BY PCA AND D-OPTIMAL DESIGN

The traditional way of performing parameter estimation generally gives good results since all experimental data is used. Long simulation time, risk of finding a local minima far from the global minima, risk of being dominated by certain parameters, and high parameter correlations are however all possible drawbacks with the method. The method with MVDA described in the current work was applied to reduce these drawbacks but with similar or better end results than for the traditional method. The methodology was an extension of the work performed by Sjöblom et al. [55].

5.4.1 METHOD

The method used for parameter estimation with MVDA is an iterative process divided into a number of sub-operations that are schematically summarized in figure 20.

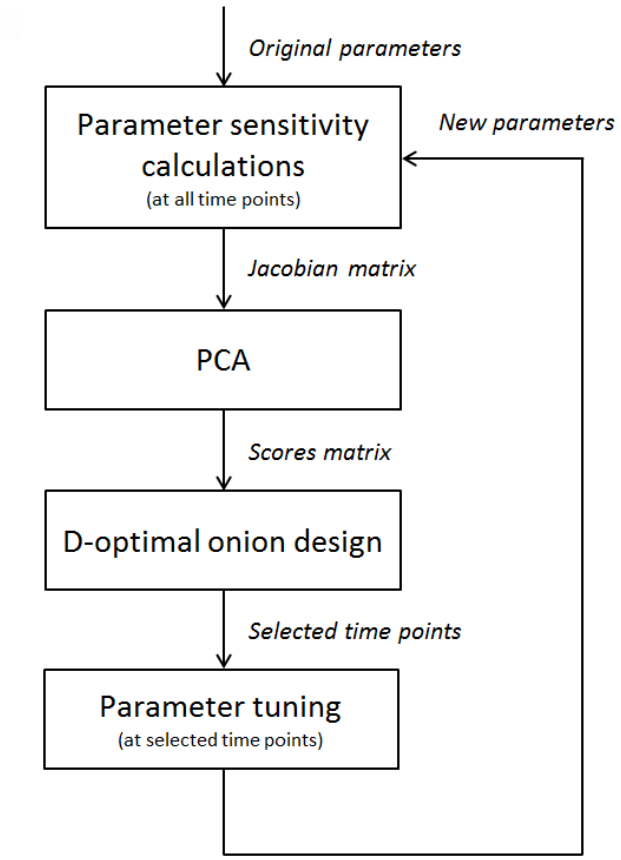

FIGURE 20 *Summary of the MVDA method of parameter estimation*

The first step in the method is the calculation of the parameter sensitivity matrix, often referred to as the Jacobian (previously introduced in equation 18). The Jacobian is not solved analytically since the system is too complex; instead it is estimated by finite differences. In the current application the Jacobian has N rows and K*P columns where N is the number of observations (time points), K is the number of responses (residual types) and P is the number of parameters.

In the second step a PCA, see section 2.1 and equation 1, is performed on the Jacobian matrix to generate a scores matrix describing the similarity in parameter sensitivity for the time points. This step is not strictly necessary since a D-optimal design could be performed directly on the Jacobian even though that would be far more time consuming.

By performing a D-optimal design on the scores matrix it was possible to identify the time points where the influence from parameter changes on the different residuals were most noticeable, that is the parameter sensitivity was

high. These time points were thereby good candidates to use if the number of time points were to be reduced. Previous studies did however reveal that a pure D-optimal design did tend to select only the most extreme points that were not very representative for the data set and thus did not improve the parameter estimation. The remedy for this problem was to instead use the D-optimal onion design, introduced in section 2.2.1, and to select a larger number of data points (approximately 1% of the total time points). The number of points per onion layer was selected to increase exponentially with decreasing sensitivity which resulted in a majority of the points being selected at high sensitivity. An example of the sectioning of the data set into layers and the relative parameter sensitivity of the data points in the layers is shown in figure 21.

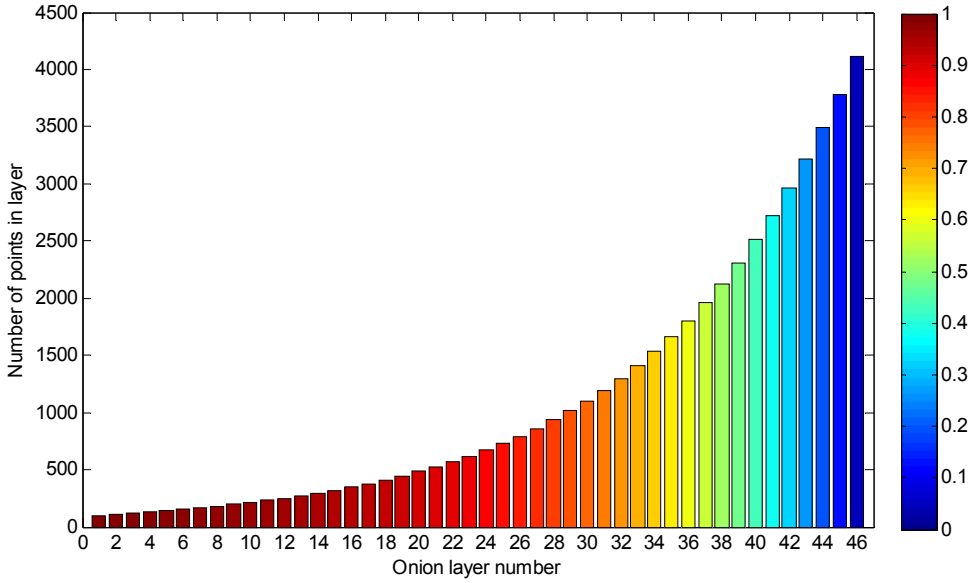

FIGURE 21 *D-optimal onion layer thickness colored by relative sensitivity. The relative sensitivity is an indication of how sensitive the data point is to changes in parameter value relative to the rest of the data set.*

The time points selected with D-optimal onion design were used for parameter estimation with a limited number of steps in parameter space (1 or 5) to avoid changing the parameters too far from the values where the Jacobian was calculated in the first step of the method. The resulting parameter set was then used to calculate a new Jacobian for the entire data set which puts the method back to the top square in the method overview in figure 20.

To summarize the principle of the method is that parameter estimation should be performed only on a limited number of time points that have a high sensitivity for parameter change and that gives a more equal influence from the different parameters on the residual. To achieve these conditions an analysis is continuously made on the system to update the point selection when new parameter values are found to ensure favorable statistical properties.

5.5 COMPUTATIONAL EFFICIENCY

Parameter estimation on highly dynamic systems such as a full scale catalyst is a computationally demanding process. The focus of this project was to evaluate different methods of parameter estimation and to make them as efficient as possible which means that a lot of computational power has been needed. Without an efficient use of the available computational resources the project would simply not be where it is today. The measures taken to improve the computational efficiency are described in the following sections.

5.5.1 PARALLELIZATION

The software used for all simulations, parameter estimations, and data analysis is numerical computing environment Matlab including Matlab Statistical toolbox and Matlab Parallel Computing toolbox.

The default setting for Matlab is to perform calculations on a single processor core which, in the case of a multi-core computer, means that the full computational power is not used. Matlab Parallel Computing toolbox, however, makes it possible to run computations in parallel over a number of processor cores, sometimes referred to as workers, on one local computer.

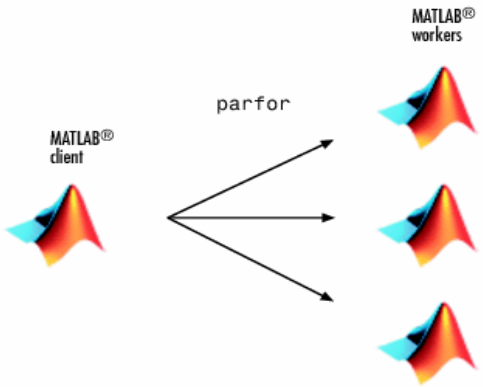

FIGURE 22 *A Matlab computation can be distributed over several processor cores (workers) by creating a parfor loop*

To make parallel computation possible the computations performed on each core need to be independent of the calculations on the other cores. For example it would not be possible to calculate the washcoat concentration of NO on one core and the washcoat concentration of CO on another core since both concentrations will influence each other's rate of reaction.

One calculation that can be divided into sub-sets of independent calculations is the Jacobian estimation with finite difference. This means that the residual changes of a finite step in one parameter can be calculated independently of the residual changes of a finite step in a different parameter. The parallelization of the Jacobian calculation has made parameter estimation according to figure 23 possible.

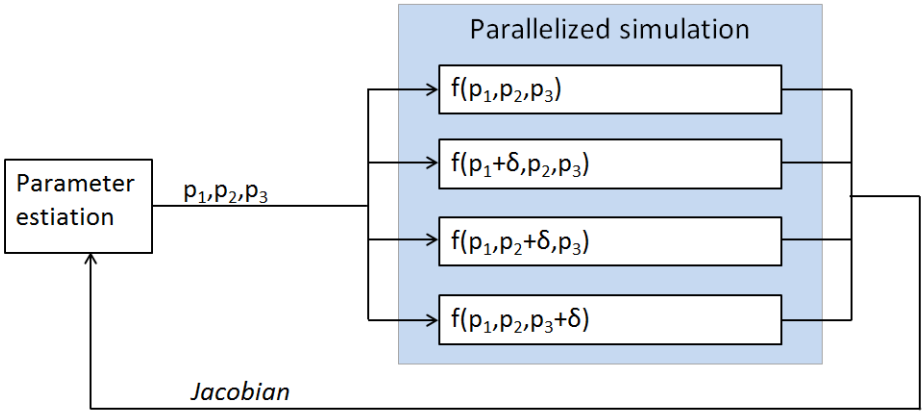

FIGURE 23 *Parallelized computation during parameter estimation illustrated by parallelization over the Jacobian calculation for three parameters (p_1, p_2, and p_3) where δ is finite difference and f is the residual function.*

In figure 23 the principle for estimating three parameters parallelized was shown where the number of available cores for optimal computational time

was equal to the number of parameters plus one. In theory the reduction in total estimation time would be of the same order as the number of cores used but in reality it is somewhat lower due to shared computational resources between the cores.

5.5.2 CLUSTER COMPUTATION

The number of available cores per cluster computer used in the current work was 16. This means that the optimal number of parameters to estimate would be 15 since one core is needed to calculate the residuals for the unmodified parameter values. For the final study the number of parameters was 18 but to evaluate the optimization possibilities an algorithm where three random parameters at a time were omitted from the Jacobian calculation was created. The algorithm achieved a faster reduction in residual than the traditional method but was not evaluated enough to determine if an equally good final fit could be achieved.

6 RESULTS AND DISCUSSION

The results and discussion is divided into two sections where the first section presents the studies in Paper I and II and the second section presents the results from Paper III, IV and from the parameter estimation from Scania engine rig data. As presented in the introduction (section 1.5) these two sections represent two approaches to engine rig parameter estimation. The first approach used only full scale experiments from a standard engine rig and a global kinetic model whereas the second approach used both lab-scale and full scale experiments and a detailed kinetic model. The results are only briefly summarized to serve as a basis for discussion, for a more thorough presentation the reader is referred to the enclosed papers.

6.1 ENGINE RIG ONLY APPROACH

The two studies performed with the Engine rig only approach used the same experimental data but differ in objectives. The first study (Paper I) focused on the modeling of mass transport in the washcoat and the necessity of including it in the model while the second study (Paper II) evaluated the possibilities of improving the fit of the model by including MVDA in the parameter estimation process.

The experimental set-up and experimental plan including catalyst configurations and engine operating points were described in section 3.2. The catalyst model and discretization were described in section 4.1 and the global kinetic model used was described in section 4.2. It should here be stressed that the parameter estimation performed in these studies involved a retuning of

kinetic parameters taken from previous studies. It was not an estimation from theoretical parameter values based on elementary reactions.

The heat transfer parameters thermal mass, environmental temperature, and lumped heat transfer coefficient were tuned before any additional parameter tuning was performed in the first study. The resulting parameter values were used in the second study as well.

6.1.1 EVALUATION OF INTERNAL MASS TRANSPORT MODELING

Two of the catalyst configurations in the experimental plan had the same platinum loading (15 g/ft^3) but different washcoat thicknesses, see table 1. It should thereby be possible to distinguish effects of transport resistance in the measurement data directly. To do this the conversion of NO, HC and CO were plotted against temperature and compared. No clear indications were found for HC and CO which was probably the result of a lack of data, especially at low conversions. For NO the trends were clear which can be seen in figure 24 where NO conversion in relation to conversion at thermodynamic equilibrium is shown for the two catalyst configurations.

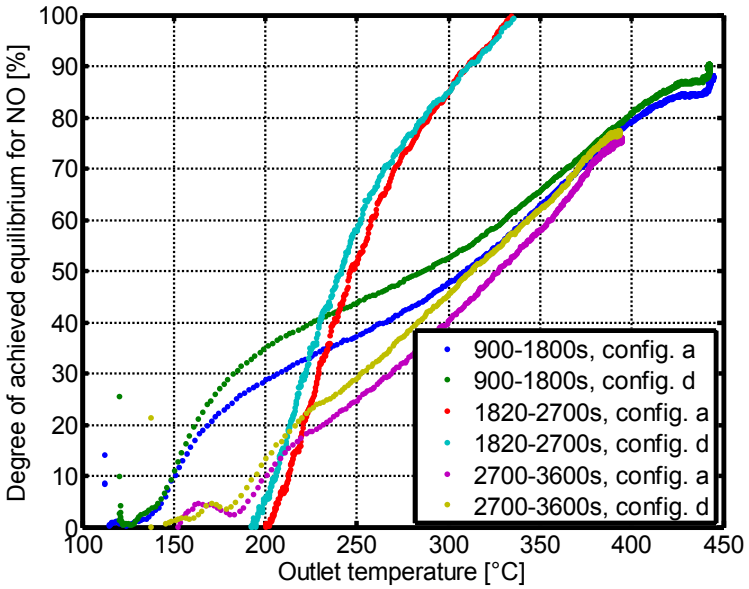

FIGURE 24 *Measured degree of achieved equilibrium for NO for two catalyst configurations (see table 1) with same platinum loading but different washcoat thickness. Time intervals are taken from the total experimental data.*

The time intervals in the legend of figure 24 are taken from the total experimental data and configurations a is the catalyst with the thicker washcoat and catalyst d is the catalyst with the thinner washcoat.

The thinner washcoat of catalyst configuration d results in lower internal transport resistance than for catalyst configuration a. This results in a higher conversion for catalyst configuration d if internal mass transport limits the reaction rate. When the three different temperature transients in figure 24 are compared it is apparent that the conversion was indeed higher for catalyst configuration d at certain temperatures. At lower temperatures the conversion was limited by kinetic reaction rate which means that only the platinum loading was of influence and not the transport resistances. As the temperature increased the influence of internal transport resistance also increased which can be seen as a difference in conversion between the two catalyst configurations for all three transients at temperatures above 200 °C. This difference was most pronounced for the transients taken between 900 s and 1800 s but was also clear for the two other transients. At even higher temperatures the reaction rates increased to a point where the thermodynamic limits were reached giving a more equal conversion for the catalyst configurations. The fact that the conversions were equal at low temperatures is a good indication that the difference in conversion when the temperature was increased is not attributed to a difference in dispersion but rather to internal transport resistance. Similar effects due to internal mass transport limitations, but for NO conversion during SCR, has been reported by Metkar et al. [60] and Nova et al. [61].

Three different modeling approaches, called modes in the study, were used for parameter tuning. The three modes were defined to evaluate the effects of including internal transport resistance in the catalyst model and the effect of tuning mass transport parameters, the modes are summarized in table 7.

TABLE 7 *Short description of the modes of parameter estimation*

Nr.	Modes of parameter estimation	Number of parameters	Discretization	
			Segments	Layers
1	Negligible internal mass transfer resistance	17	10	8*
2	Fixed effective diffusivity	17	10	8
3	Tuned effective diffusivity	19	10	8

*Since no concentration gradients in the washcoat were expected two layers would have been enough for this case, however eight layers were used for computational consistency

Mode 1 represents a case where the effective diffusivities were set to very high values (1000 times initial estimates) which, in effect, makes it a case with negligible internal transport resistance. Mode 2 and Mode 3 differ only by the fact that the latter had enabled estimation of the effective diffusivity whereas the former had not. For Mode 2 the effective diffusivities were fixed at the initially estimated values. Mode 3 used one effective diffusivity scaling factor for small molecules and one for large molecules where all components except HC were considered small (see section 0 for more details on mass transfer parameter estimation).

The result of the parameter tuning is shown as residual sum of squares for NO, HC, CO and NO_2 in table 8 where the definition of the residuals was according to section 5.3.1.

TABLE 8 *Residual sum square ($\times 10^5$) of every component together with the summation of residual sum square (rightmost column) for the different modes.*

	NO	**HC**	**CO**	**NO_2**	**Sum**
Mode 1	0.67	3.10	4.46	0.83	9.05
Mode 2	2.09	2.44	6.89	2.64	14.1
Mode 3	0.77	2.41	3.49	0.97	7.65

The most striking result from table 8 is that the fit of the model with no internal transport resistance gave a residual sum of square that was not very far from the model where the transport resistance was tuned. There may be several reasons for this but the most important one is likely associated with the structure of the global kinetic model used.

If the activation energies of the starting parameters (section 4.2.1) are studied it can be noted that $E_{A,7}$ stands out since it has a positive sign opposite to the other activation energies in the denominator. This means that the inhibition by NO will increase with temperature and that this factor will result in a reduction of the reaction rate with temperature. In other words, it is the same kind of phenomena that transport resistance would cause and gives the kinetic model the ability to model the effect of mass transport even if it is not included in the catalyst model definition. It is not physically realistic for an adsorption enthalpy to be endothermic, thus it is questionable whether the term $K_7 y_{NO}^{0.7}$ truly accounts for NO inhibition. The starting kinetic parameters

were collected from lab-scale data, where the transport resistance was assumed to be negligible. It may be speculated that the difficulties encountered when tuning a model where the transport resistance is not neglected could indicate that the original parameters were in fact influenced by transport resistance, a phenomena observed previously [62]. In a model that clearly separates mass transport and kinetics, it is in other words both important to have original parameters uninfluenced by transport resistance and that the kinetic model itself is not constructed to mimic internal transport effects.

Mode 3 that included parameters to tune the internal mass transport resistance did, however, give the best fit to measurement data. This shows that including internal mass transport in the model still gave the best conditions for parameter estimation but only if parameters to tune the mass transport resistance were also included.

6.1.2 MVDA METHOD

To evaluate if a better fit to measurement data could be achieved with the MVDA method, introduced in section 5.4, than a traditional method a new parameter estimation was performed. The data was the same as in previous section and the model corresponded to the previously introduced Mode 3 which meant that internal mass transport resistance was modeled and also tuned by two parameters.

Two approaches to the MVDA method were evaluated in the study. The first approach (referred to as “1 step”) selected new time points after every step in parameter space while the second approach (referred to as “5 steps”) took five steps in parameter space before new time points were selected. The difference in performance between the two approaches were, however, small and to reduce complexity only the first is included in this summary.

As discussed in section 5.3.1 the residual definition was changed from being based on concentration to be based on conversion to better suit the continuously changing selection of data points on which parameter estimation was performed. A large fraction of the data was close or equal to 100% conversion, especially for HC and CO, since many of the engine operating points chosen had high temperatures. It is not desirable to fit parameters to data points with close to 100% conversion, since the kinetic parameter

sensitivity for these points is very low. Therefore it was necessary to set the residuals to zero for certain components at such points in the data set which was another update to improve the parameter estimation compared to the preceding study (Paper I).

The data point selection with D-optimal onion design was updated as the parameters were estimated according to the method described previously. Figure 25 shows one example of a selection from which it is clear that certain areas were frequently selected from the onion layers with high sensitivity, whereas other areas were mainly selected from the onion layers with low sensitivity. The relative sensitivity depicted in figure 25 is an indication of how sensitive the data point was to changes in parameter value relative to the rest of the data set. A value of 0.9 for example, means that the data point had a higher sensitivity than 90% of the data set.

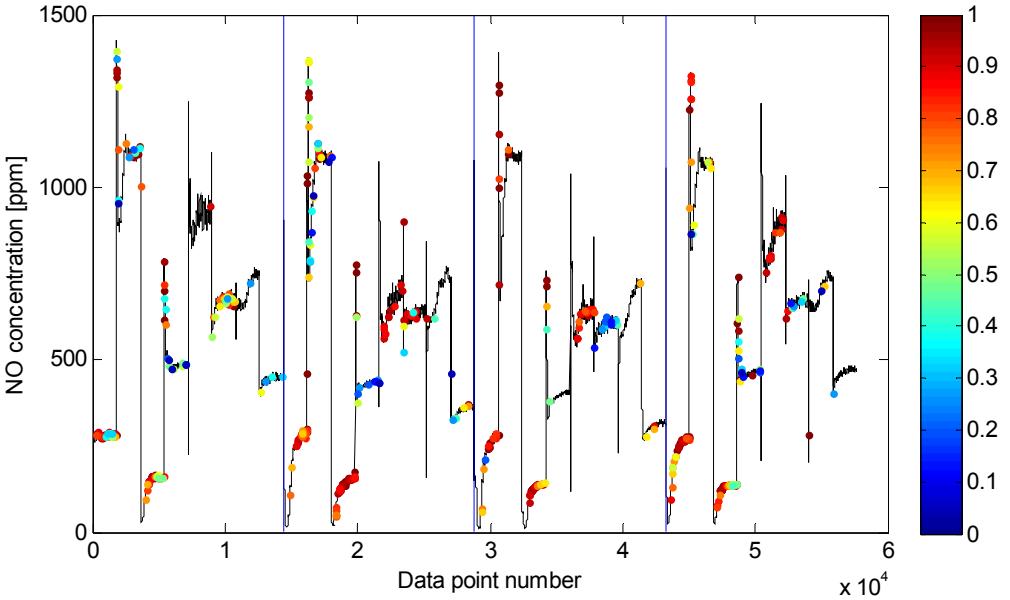

FIGURE 25 *Measured outlet mole fraction of NO for an example of a selected data set colored by relative sensitivity. The order of the engine operating points is 1, 7, 2, 8, 3, 4, 5, 6 which were run sequentially for catalyst configurations a, b, c and d (separated by blue vertical lines).*

The points selected were similar for the different catalyst configurations even though points from catalyst configuration c (data points 28818 to 43240) were less frequently selected for the depicted case. The points selected were taken from both transient and stationary sections of the data. As expected the

data points selected in layers with high sensitivity were mainly taken from transient areas while data points selected in layers with low sensitivity were mainly taken from more stationary areas.

In figure 26 the evolution of the residual sum of squares of the gas phase components (NO, HC, and CO) for the whole data set is shown. The figure also shows the final residual sum of squares for a reference case where parameter estimation was performed the standard way but with the updated residual definition.

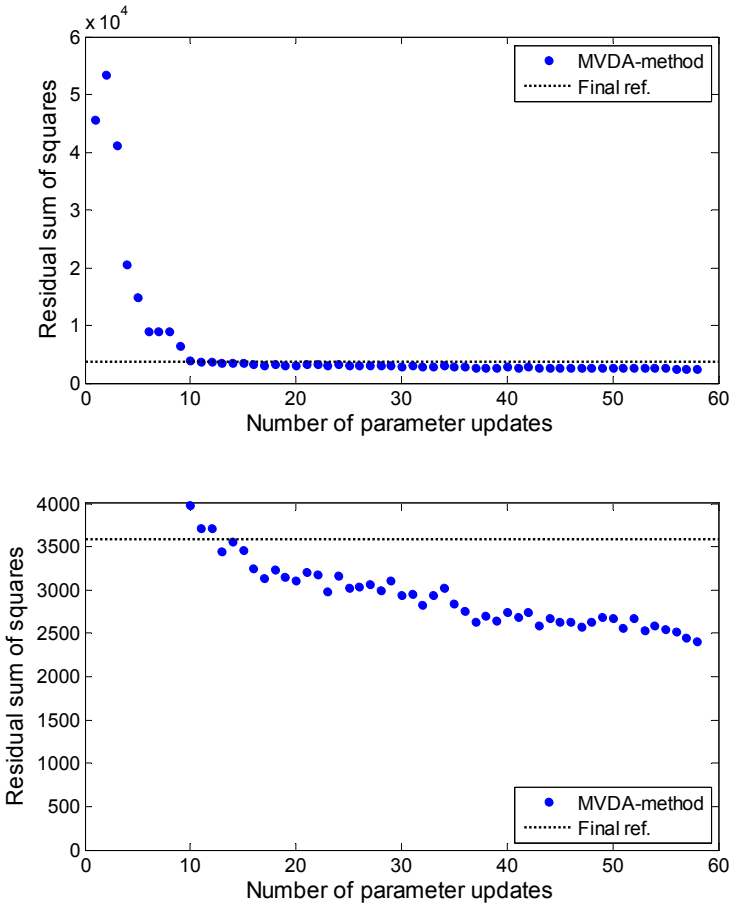

FIGURE 26 *Residual sum of squares for every set of parameters for the MVDA method. The dashed line is the residual sum of squares for the final set of parameters from the reference method. The lower frame is a magnification of the upper frame.*

The residual sum of squares for the whole data set was only calculated after a completed parameter estimation in the time points selected by D-optimal onion design.

For the reference case, the parameter estimation came to a halt after about 5×10^3 core hours of simulation with a residual sum of squares of 3580. The reference parameter tuning method was then approaching parameter values where the catalyst model was unable to find a stable solution and thereby converging to a local minimum. After 5×10^3 core hours of simulation the MVDA method had a residual sum of squares of 8919. It is therefore not possible to conclude that the MVDA method enabled a faster residual reduction. Instead the advantage with the MVDA methods appears to be a reduced risk of converging to a local minimum. Even after the comprehensive parameter tuning already performed, the residuals in figure 26 still show a declining trend even when the method has reached a residual sum of squares below 2500. Although the rate of decline appears to be decreasing, no clear optima appeared to have been reached.

6.1.3 COMPARISON TO MEASUREMENT DATA

The parameter values that gave the lowest residual sum of squares shall be regarded as the final tuning results of the method. A compilation of the residual sum of sqares for the final results and the starting paramter values are shown for every gas phase component in table 9. The results from Mode 3 in the first study have been used to recalculate the residual sum of squares with the residual definition used in the MVDA study to allow direct comparison.

TABLE 9 *Residual sum square of each component and complete data set together with the summation of residual sum square (rightmost column) for the different methods.*

	NO	**HC**	**CO**	**Sum**
Start	18986	9736	16954	45675
1 step	515	1161	730	2405
Ref*	1238	1173	1169	3580
Mode 3	1124	1103	895	3123

* reference case where parameter estimation was performed the standard way but with the residual definition used in the MVDA study

The first notable observation from table 9 is that a better fit was achieved with the standard method of parameter estimation if the residuals were defined with concentrations (as described in 5.3.1) instead of conversions (as described in 5.3.2). This again confirms the importance of defining the residuals according to the modeling purpose. In the first case the residuals were

designed to suit the standard method while the latter case was mainly designed to suit the MVDA method.

From these results it appears that HC was the most difficult component to fit to measurement data for the MVDA method which may have several different reasons. Firstly HC and CO concentrations are highly correlated in the exhaust of a HDD engine which means that it can be difficult to generate experimental data, let alone subsets of data, where the parameters that influence each component can be distinguished. Since both components have high concentrations at similar time points, the larger residual for CO at the starting parameters may have influenced the parameter estimation to initially focus more on reducing the CO residual at the cost of decreased sensitivity for HC concentration. HC also differs from NO and CO since it was modeled as an average of a wide range of hydrocarbons. The physical properties are more difficult to model and the HC composition at the catalyst inlet will even change between different engine operating points.

An example of the final results of the tuning of the kinetic and mass transport parameters for the different parameter estimation methods are shown in figure 27.

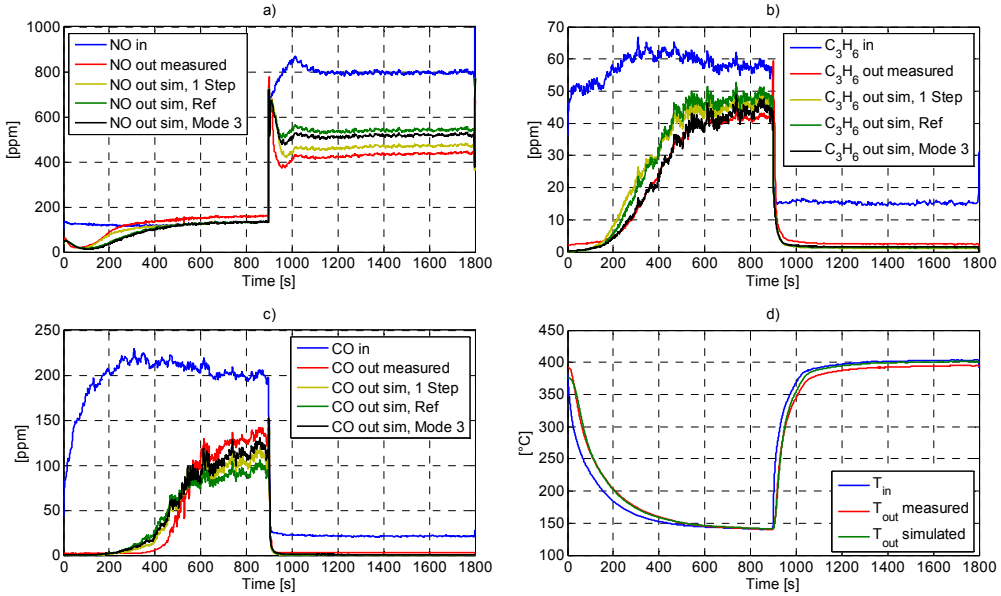

FIGURE 27 *Measured and simulated outlet concentrations of NO (a), C_3H_6 (b), CO (c) and temperature (d) for a change in operating point from 1 to 7 for catalyst configuration c.*

Figure 27 shows that the MVDA method has the best fit for NO with a wide margin but that the fit for HC was best for the parameter estimation

performed in the preceding study (Mode 3). The NO production before the change in engine operating point was likely a result of NO_2 reduction by CO or HC. These reactions were not included in the kinetic model and could therefore not be captured by any of the models. The transients in figure 27 was one of four different transients for one of the four different catalyst configurations which means that it was only 1/16 of the total data set used for parameter estimation. The figure does, however, represent residuals from the entire data set shown in table 9 quite well, with the improved fit of NO being the main strength of the parameter set estimated with the MVDA method.

6.1.4 FINAL PARAMETER VALUES

Some interesting features of the final parameters will be discussed here but for specific values the reader is referred to Paper II which includes all parameters for the simulations in the previous section. As previously observed the sign of $E_{A,7}$ in the starting parameters (see section 4.2.1) made the NO inhibition term mimic internal transport resistance since an increase in temperature reduces the reaction rate for all reactions. The sign of $E_{A,7}$ was still positive for all evaluated methods but for the MVDA method $E_{A,5}$ has changed from a negative starting value to a positive final parameter value. This means that the MVDA model had two terms mimicking internal transport resistance, one as a function of NO concentration and the other as a function of HC concentration, compared to that for the reference case.

These values together with the decreased mass transport resistance due to increased diffusivity scaling parameters meant that the actual transport resistance in the model was reduced and replaced by a fictitious one connected to the kinetics. The result of the parameter tuning with MVDA shows the importance of having a well formulated model and also displays how an efficient parameter tuning method can tune the parameters to less realistic values, and still achieve a good fit, even if the model formulation is deficient.

In general the parameter values from the preceding study (Mode 3) were closer to the values of the MVDA methods than the reference case (Ref). In addition to the residual difference a ten times higher parameter weighting for kinetic parameters (see equations 8 and 12) was used in the second study to

make the Jacobian less sensitive to numerical noise. It appears that this increased parameter weighting has resulted in estimated parameter values further away from the original ones for the reference case with an overall poorer fit. This could be an effect of some parameters having a large influence on the fit at an early stage of the parameter estimation which makes them change fast and thereby reach values where the sensitivity for the other parameters were low. In other words the risk of finding a local minimum may have increased by the increased parameter weighting. One of the aims of the MVDA method was to make the influence of parameters more equal and it appears that this has prevented the parameters from reaching extreme values for the method even though the parameter weighting was high.

6.2 MULTI-SCALE EXPERIMENTAL APPROACH

In this section the results of the Multi-scale experimental approach on efficient parameter estimation is presented. The first section includes the results from the development of a catalyst model from lab-scale experiments (Paper III) and the second section includes results from the Scania engine rig experiments (Paper IV). Both these studies have been introduced in previous sections (3.3, and 3.1.2, 3.4 and 4.2.2) including some results and the results presented here will therefore be brief. To conclude the Multi-scale experimental approach some parameter estimation results are presented where the parameters from the lab-scale pre-study were re-tuned to the Scania engine rig data.

6.2.1 LAB-SCALE PRE-STUDY

The objective of the lab-scale pre-study was to develop a kinetic and transport model for a DOC that obtained a satisfactory compromise between accuracy, computational demands and robustness for simulation of transient full-scale operation. Specifically the model should account for surface concentrations of key species needed to capture transient kinetic features for typical lean exhaust engine conditions. In addition, the model should properly account for transport limitations and distinguish them from reaction kinetics.

The structure of the kinetic model has already been presented in section 4.2.2 and was a very important output of the study. For the parameter

estimation half of the experimental data was used in the parameter estimation process and half of the data was used for verification. The experiments used for parameter estimation were selected with the principle that the three different inert washcoat loadings (table 2) should be represented for every experimental type (table 4). The tuned catalyst model showed good agreement with measured conversion levels for the light-off experiments and inert washcoat thicknesses indicating a successful separation of mass transport and kinetics. The main purpose of the model was however to be used for more complex gas mixtures. To demonstrate the performance of the model at more engine like conditions the simulation of one of the so called full gas mix experiments is shown in figure 28.

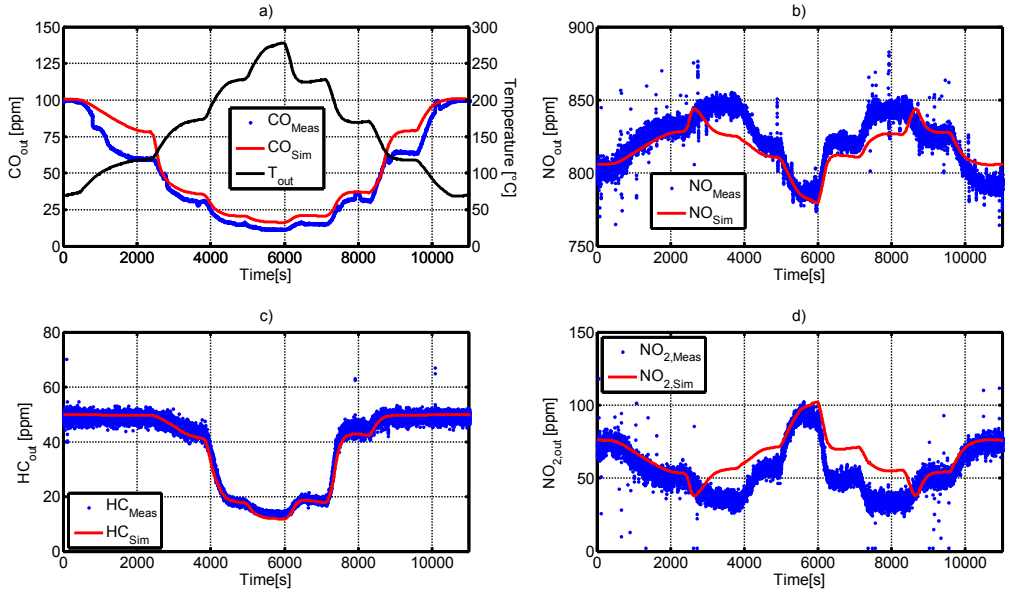

FIGURE 28 *Experimental and simulation results for full gas mix for catalysts 6 (see table 2) with 5 g/ft³ platinum loading and 2 g/inch³ inert washcoat loading. The inlet concentrations were 100 ppm CO, 800 ppm NO, 50 ppm HC and 80 ppm NO_2.*

Overall the fit is very good even though the simulated CO concentration is somewhat higher than the measured values around 2000 s. To evaluate the kinetic model the surface coverages and the reaction rates for oxidation of CO and HC are shown in figure 29.

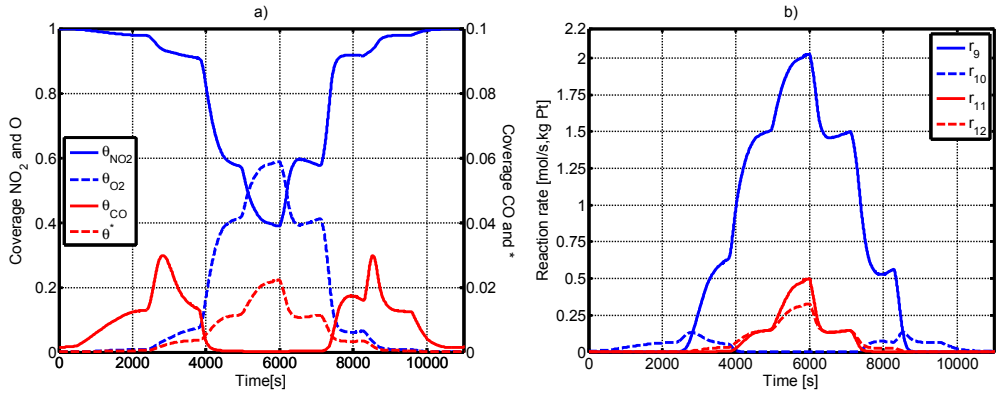

FIGURE 29 *Simulation results of full gas mix experiment with catalyst 6 a) coverages b) reaction rates for oxidation of CO and HC*

As the analysis of the experimental data suggested in section 4.2.2, NO_2 is initially the most active oxidant giving it a dominant surface presence at low temperature. This is also seen in panel b) in figure 29 where CO oxidation by NO_2 (r_{10}) is the fastest reaction during the first (and last) 3000 s. Due to the high NO_2 coverage, the CO coverage will remain low throughout the experiment and thereby negate any CO poisoning effects. As the temperature increases the oxygen coverage increases as reactions with oxygen as oxidizing species (r_9 and r_{11}) take over as the fastest reactions. The role of HC oxidation by NO_2 (r_{12}) is difficult to identify from the measurement data but from the simulation results it appears that the reaction becomes active at the same temperature as the regular oxidation of HC by oxygen (r_{11}). Since CO is oxidized only by oxygen at the temperatures where r_{12} is active, the reaction may be necessary to achieve NO_x concentrations that agree with the experimental data.

6.2.2 SCANIA ENGINE RIG

In this section two examples of results from experimental types 2 and 3 described in section 3.3.2 are shown as a demonstration of the exhaust gas compositions made possible by the Scania engine rig set-up.

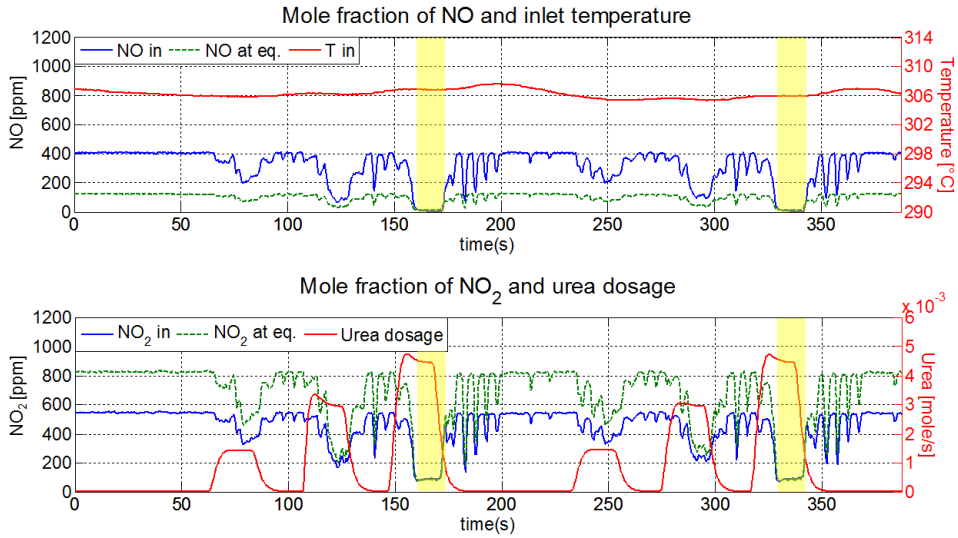

FIGURE 30 *NO and NO_2 concentrations, and temperature in the test object inlet, and urea dosage for one experiment of type 2. Green dashed lines show the thermodynamic equilibrium concentrations for the NO oxidation reaction. Yellow marking show NO concentrations close to zero.*

In figure 30 one experiment of type 2 is shown. In this type of experiment the SCR and urea injection makes it possible to achieve a wide range of NO_2/NO_x ratios and concentrations. Two cycles with increasing urea dosage (0%, 30%, 60% and 90% of stoichiometric NO_x reduction) were performed in the experiment. For the results shown in figure 30 valve 2 was closed and valve 1 was fully open (see figure 11 for engine rig layout). A NO_x composition containing close to 100% NO_2 can be observed at high urea dosages for some cases (see yellow marking in figure 30). CO and HC concentrations are not shown since the conversions of these components were always close to 100 %.

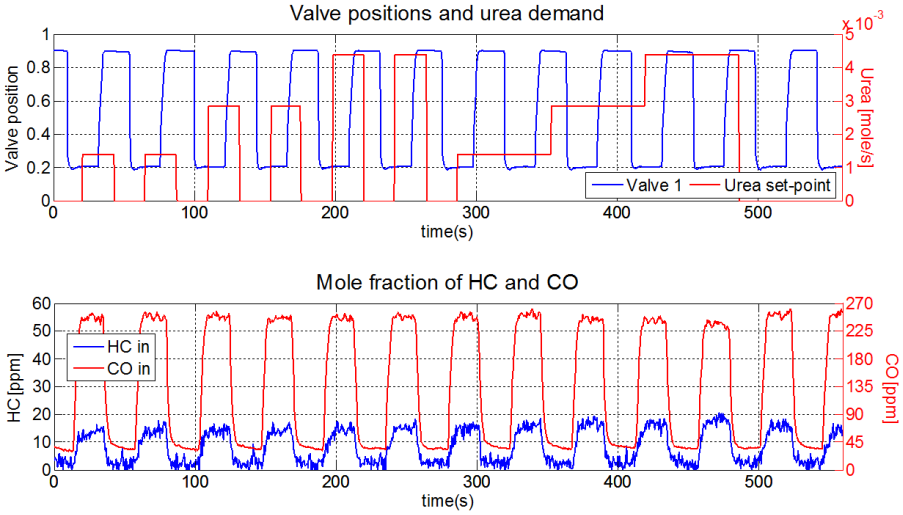

FIGURE 31 *HC and CO concentrations, valve 1 position, and set-point for urea dosage for one experiment of type 3*

Figure 31 and figure 32 show the results of one experiment of type 3. Figure 31 shows sequences where the CO concentration was high at the same time as the HC concentration was close to zero. This behavior is even more pronounced for experiments performed at engine operating points with higher exhaust temperatures. Figure 31 also shows that both HC and CO were unaffected by the urea injection.

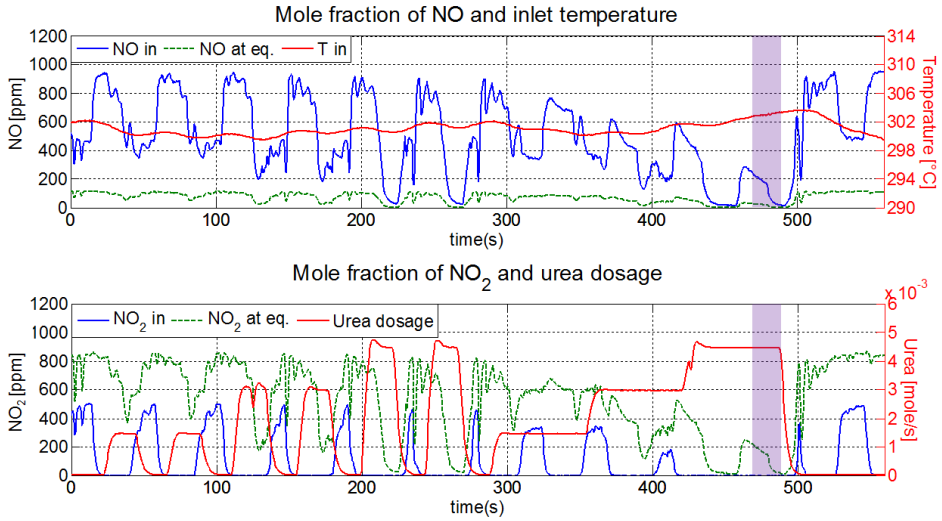

FIGURE 32 *NO and NO_2 concentrations, temperature, and urea dosage for one experiment of type 3. Green dashed lines show the thermodynamic equilibrium concentrations for the NO oxidation reaction. Purple markings show time range where CO concentration exceeds NO_x concentration.*

Figure 32 shows that NO and NO_2 were affected by both the urea injection and the DOC bypass ratio. At high urea injection all NO_2 and most NO were consumed.

6.2.3 PARAMETER ESTIMATION

With the kinetic model presented in the lab-scale pre-study (section 6.2.1) a new parameter tuning was performed on a selection of the experiments from the engine rig set-up presented in section 3.3. The results presented in this section are preliminary and the parameters shown represent the best fit at the printing of this thesis. The parameter tuning process has not converged and the most favorable settings for the parameter estimation, such as residual definition and experimental selection, may not have been found. Nevertheless some results are presented to conclude the Multi-scale experimental approach.

For the parameter tuning, four experiments of each type (see section 3.3) were used giving 12 experiments in total. The result from one experiment of type 2 is shown in figure 33.

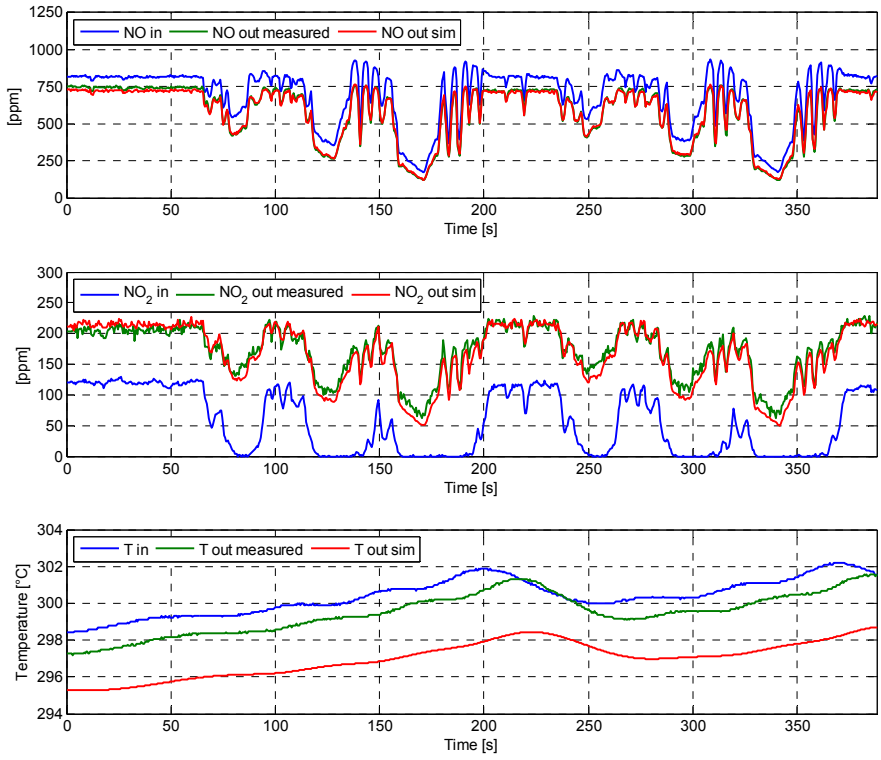

FIGURE 33 *Parameter estimation result of one type 2 experiment with a full scale 5 g Pt/ft^3 catalyst with no inert washcoat layer (catalyst e in table 1)*

The model showed a good fit to experimental data for NO and NO_2 even though the model appears to have overestimated the NO conversion to NO_2 somewhat. To also evaluate the fit of HC and CO one experiment, of type 3 is shown in figure 34 and one experiment of type 1 is shown in figure 35.

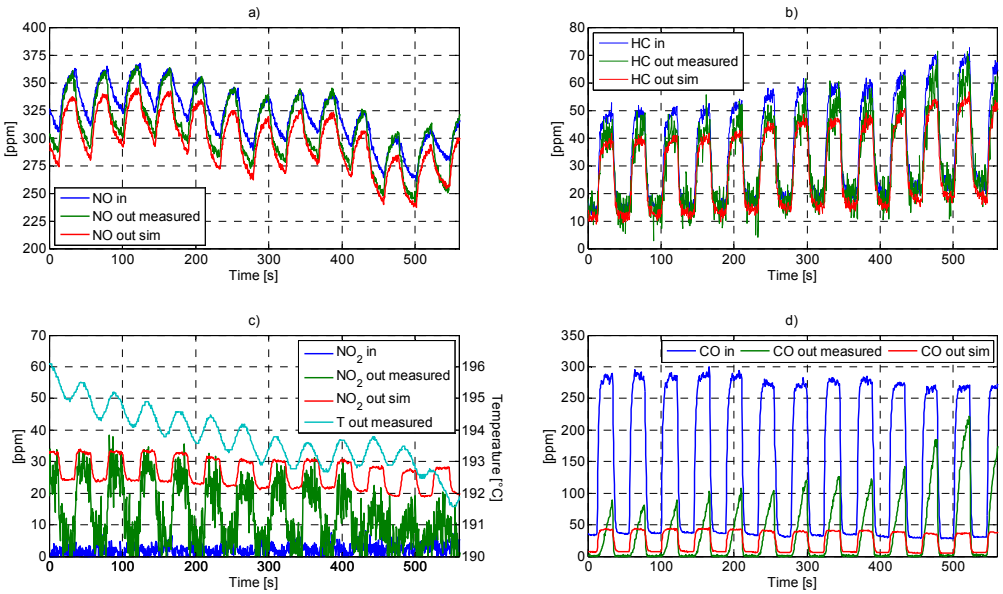

FIGURE 34 *Parameter estimation result of one type 3 experiment with a 5 g Pt/ft³ catalyst. Measured T_{out} is considered to describe the temperature transients in the catalyst adequately since it is within 2°C from both simulated T_{out} and measured T_{in}.*

Panels b) and d) in figure 34 show that the model overestimated both the HC and CO conversion. The measured CO showed a decreasing conversion with time at high CO levels. This could be an effect of decreasing temperature since the temperature was close to the light-off temperature observed in the lab-scale experiments, see figure 18. There is, however, also a possibility that the trend was a result of competitive adsorption. Neither of these phenomena was described well enough by the model at the current stage of the parameter tuning process.

The low temperature in figure 34 means that NO oxidation in the upstream DOC was low and thereby the effect of the urea dosage was less than in the experiment shown in figure 32. The model also has difficulties reproducing the behavior of the NO conversion where the model predicted a near constant NO conversion while the measurement switched between zero conversion and what was predicted by the model, see panel a). The low measured conversion of NO coincides with high concentrations of both HC and CO which indicates that these components may have inhibited the NO oxidation. The source of the inhibition could be both competitive adsorption and NO_2 reacting as oxidizing agent.

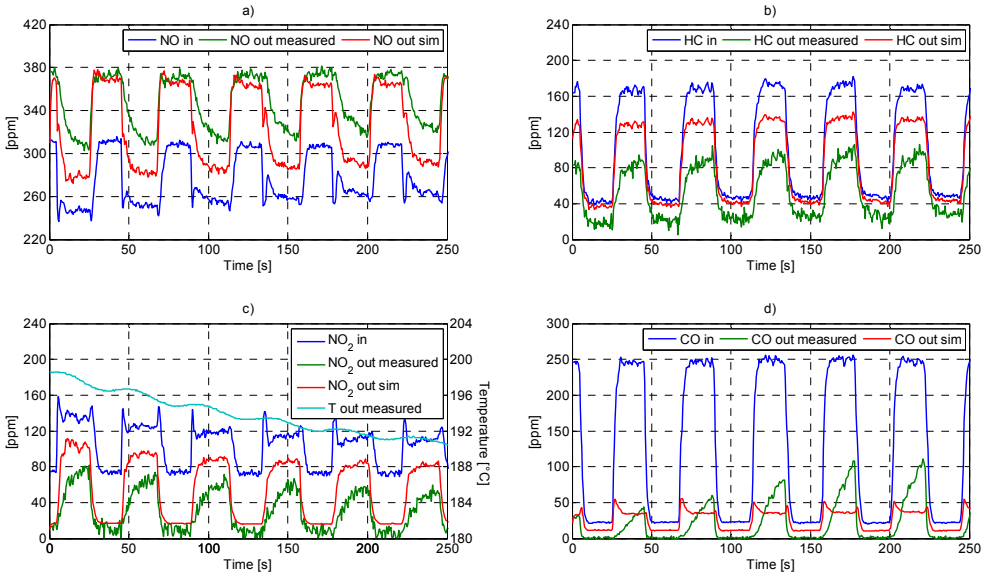

FIGURE 35 *Parameter estimation result of one type 1 experiment with a 5 g Pt/ft³ catalyst. Measured T_{out} is considered to describe the temperature transients in the catalyst adequately since it is within 2°C from both simulated T_{out} and measured T_{in}.*

The CO conversions in panel d) in figure 35 show a similar trend to what was observed for the experiment of type 3 in figure 34 that had similar temperature. Both the HC conversion and the NO_x concentrations are, on the other hand, distinctively different. NO was formed and NO_2 was consumed for all time points (panels a) and c)) and the measured HC conversion was higher than the modeled (panel d)). The kinetic model was able to reproduce this behavior but the fit is not as good as in previously presented simulations.

For the model to reproduce the measured outlet concentrations when the inlet NO_2 concentration was at the higher levels almost all HC and CO would need to be oxidized by NO_2. This was clearly not the case since the modeled HC conversion was close to 0% when the NO_2 inlet concentration was high. The reaction between NO_2 and HC did however take place in the model at the lower NO_2 inlet concentrations and was also the reason why the simulated conversion of HC was higher than in the experiment in figure 34. Even though the fit to measurement data could be improved the data clearly indicates the necessity of including both oxidation of CO and HC by NO_2 in the model.

The final parameter values of the parameter tuning are shown in table 10 together with the parameters from the lab-scale pre-study.

TABLE 10 *Final parameters from full scale parameter tuning compared to parameters from lab-scale pre-study*

Tuned parameters					
	Pre-study	**Full scale**		**Pre-study**	**Full scale**
$\mathbf{A_2}$	2.08×10^{7}	5.10×10^{6}	$\mathbf{E_{A.2}}$	5.61×10^{4}	5.07×10^{4}
$\mathbf{A_4}$	1.32×10^{8}	3.09×10^{7}	$\mathbf{E_{A.4}}$	5.02×10^{4}	4.93×10^{4}
$\mathbf{A_5}$	1.70×10^{5}	3.15×10^{5}	$\mathbf{E_{A.5}}$	3.39×10^{4}	3.08×10^{4}
$\mathbf{A_6}$	1.33×10^{10}	1.16×10^{10}	$\mathbf{E_{A.6}}$	1.25×10^{5}	1.24×10^{5}
$\mathbf{A_8}$	6.15×10^{16}	1.14×10^{15}	$\mathbf{E_{A.8}}$	1.61×10^{5}	1.50×10^{5}
$\mathbf{A_9}$	2.05×10^{14}	2.18×10^{18}	$\mathbf{E_{A.9}}$	9.91×10^{4}	1.31×10^{5}
$\mathbf{A_{10}}$	30.5	4.39×10^{2}	$\mathbf{E_{A.10}}$	3.32×10^{3}	1.38×10^{4}
$\mathbf{A_{11}}$	2.44×10^{8}	6.56×10^{2}	$\mathbf{E_{A.11}}$	5.08×10^{4}	5.00×10^{3}
$\mathbf{A_{12}}$	1.38×10^{13}	3.82×10^{10}	$\mathbf{E_{A.12}}$	1.03×10^{5}	8.34×10^{4}
$\mathbf{f_{Dscl,S}}^{\dagger}$	14.4	6.96	$\mathbf{f_{Dscl,L}}^{\dagger}$	12.4	5.35
Fixed parameters					
$\mathbf{A_1}$	2.49×10^{6}		$\mathbf{E_{A.1}}$	2.10×10^{4}	
$\mathbf{A_3}$	2.86×10^{7}		$\mathbf{E_{A.3}}$	0	
$\mathbf{A_7}$	5.44×10^{3}		$\mathbf{E_{A.7}}$	0	

† Effective diffusivity scaling for small (S) and large (L) molecules

If the pre-exponential factors and activation energies are studied it can be concluded that most tuned parameters are close to the original values from the pre-study. The most noteworthy exceptions are the parameters influencing reaction 10 and 11. Reaction 10 is the oxidation of CO by NO_2 and in the lab-scale pre-study it was concluded that the experimental data available did not give the best conditions for modeling this reaction. This was also confirmed by large confidence intervals. It is therefore not surprising that the parameters have changed significantly when tuned to a different data set.

Reaction 11 is the oxidation of HC by O_2 and compared to the parameters from lab-scale the tuned parameters have considerably lower pre-exponential factor and activation energy. This is likely a result of a lack in complexity in the experimental data chosen for parameter tuning. The experimental data where the conversion for HC is high also has high conversion for CO and a production of NO from NO_2. This means that it is difficult to distinguish if the produced NO is a product of CO or HC being oxidized. From the tuned kinetic model it appears that HC is mainly oxidized by NO_2 while CO is oxidized by both O_2 and NO_2. For the experiment in figure 35 oxidation of HC by both O_2 and NO_2 does however appear to be necessary which indicates that further parameter estimation may increase the importance of O_2 oxidation of HC.

7 CONCLUSIONS

The conclusions will be divided into three parts where the first part is the conclusions from the Engine rig only approach and the second part is the conclusions from the Multi-scale experimental approach. The third part is a short summary of lessons learned along the way that did not end up in any of the scientific results.

7.1 ENGINE RIG ONLY APPROACH

Several conclusions could be drawn from the parameter estimation performed in Paper I and II both regarding modeling and parameter estimation. The most important conclusion from Paper I was that the best fit with a catalyst model with internal transport resistance could be achieved if some parameters affecting the internal mass transport (in this study effective diffusivity) were tuned in addition to the kinetic parameters. This indicated that internal transport limitations is of importance for a DOC in a heavy-duty vehicle aftertreatment system.

The study also showed that it is still possible to obtain a good fit for a model with negligible internal transport resistance since kinetic parameters could compensate for transport limitations. This highlighted the inherent difficulties using kinetic models with high parameter correlation and also showed the importance of using a kinetic model that has an intrinsic kinetic structure.

The parameter estimation performed with the MVDA method presented in Paper II displayed a better overall fit for all components resulting in a residual sum of squares 32% below what was achieved with a conventional method used as reference. The method displayed less tendencies to converge to local

minima and to reach areas where the catalyst model was unstable, however, the method was more computationally expensive than the reference method.

7.2 MULTI-SCALE EXPERIMENTAL APPROACH

The conclusions from the lab-scale pre-study were either based directly on the experimental results or were a product from the process of creating a detailed kinetic model.

The light-off experiments and the gas mix experiment with different catalyst configurations showed that NO_2 is a stronger oxidizing agent than O_2 and plays an important role at low temperature (<120°C). The experimental data also showed a clear effect of increased transport resistance for HC and CO but it was also observed for NO.

From the modeling the most important conclusion was that a good fit to measurement data could be achieved with a model using surface adsorbed atomic oxygen, CO and NO_2, but not hydrocarbons and NO. The use of different thicknesses of an inert washcoat layer closest to the gas bulk also appeared to improve the conditions for separating kinetics from transport phenomena

The most apparent advantage with the experimental set-up of the Scania engine rig was the possibility to achieve fast transients in concentration with only small variations in temperature. Furthermore the experimental data has also shown that the following engine rig exhaust gas features were enabled by the experimental set-up that would not be possible with a standard engine rig:

- High CO concentrations with HC concentrations close to zero
- NO concentrations close to zero with significant NO_2 concentration

The reduced correlation between temperature and concentrations, but also between individual concentrations, significantly widen the possible experimental conditions available and may be of great aid in full scale parameter tuning and catalyst modeling.

The goal with the Multi-scale experimental approach was to improve the conditions for effective parameter estimation mainly by providing new

possibilities for kinetic model development. A more detailed kinetic model with less correlation between parameters and better separation of kinetics and mass transport replaced the global kinetic model from the Engine rig only approach. The full scale data was also generated by a more refined set-up allowing variables (concentrations) to be varied more independently than in the standard engine rig used in the Engine rig only approach. The conclusions from the two individual studies are given above but final results and conclusion from the final study cannot be given since the parameter estimation is only initiated and not completed. Some observations can however already be made.

- The model fit for NO and NO_2 was very good in the absence of CO and HC
- Oxidation of CO and HC with both O_2 and NO_2 appeared to be important to include in the kinetic model

7.3 LESSONS LEARNED

One of the assumptions with the catalyst model used in all studies was that all catalyst channels have the same inlet conditions and that radial temperature gradients were neglected. It was therefore very important to reduce temperature gradients both in the inlet and in the catalyst itself when performing experiments. For the first experiments (Paper I and II) the gradients were notable but for the study in Paper IV extra insulation before the catalyst proved to reduce the gradients significantly. Even at lab-scale there were some indications of radial temperature gradients that could contribute to the hysteresis of NO in the light-off experiments. This problem could most likely have been prevented if the temperature transients of the lab-scale experiments were slower.

Detailed kinetic models are more suited for models where mass transfer and kinetics are to be separated but will also lead to extra stability issues for the catalyst model. Since the reactions are more correlated, through the surface coverage, than for a global model it is more challenging to find parameters that make the model stable but at the same time provide reasonable conversions. A large effort was put into evaluating different sets of starting parameters in Paper III before one was found that gave reasonable conversions for all components. In retrospect it would probably have been

more feasible to first make a comprehensive parameter screening instead of relying on the parameter estimation algorithm to tune initial parameters giving very poor fit to measurement data. This is also one of the weaknesses with the gradient search method. When the fit of a model is poor the parameter sensitivity is often low which means that the algorithm may encounter difficulties finding a direction in which the parameters should be changed to reduce the residual. The large computational effort put into finding good starting parameters also meant that not enough resources were available to evaluate the MVDA method for the parameter estimation performed in the Multi-scale experimental approach.

The experimental work in this study has been performed by the industrial partners (Johnson Matthey and Scania). This meant that the experiments were planned in detail far in advance to fit in the experimental schedules of the facilities. The advantage was that the project could focus on the modeling at the same time as the experimental work was professionally carried out. The drawback was, however, little flexibility to change the experiments as results were generated and a resulting long waiting time to perform complementary experiments.

An important lesson learned was therefore to include the need for complementary experiments in the experimental plan and to avoid trying to do all experiments for a study at one occasion. The result of not using this approach was that a considerable amount of the data had a high conversion both for lab and engine rig experiments which is not desirable for parameter estimation. In general lower platinum loadings would therefore have been better, especially in the engine rig experiments.

NOMENCLATURE

ABBREVIATIONS

ASC	Ammonia slip catalyst
CFD	Computational fluid dynamics
cpsi	Cells per square inch
DOC	Diesel oxidation catalyst
DoE	Design of experiments
DPF	Diesel particulate filter
EGR	Exhaust gas recirculation
HC	Hydrocarbons
HDD	Heavy duty diesel
MVDA	Multivariate data analysis
PCA	Principal component analysis
PM	Particulate matter
Pt	Platinum
SCR	Selective catalytic reduction

VARIABLES

A	Pre-exponential factor
C	Scores matrix
D	Gas diffusivity
$\mathbf{D_{eff}}$	Effective diffusivity
DK	Knudsen diffusivity
E	Error matrix
$\mathbf{E_A}$	Activation energy
f	Residual function
$\mathbf{f_D}$	Washcoat pore factor
$\mathbf{f_{D,scale}}$	Scale factor for f_D
G	Inhibition term in global kinetic model
J	Jacobian matrix
k	Reaction rate coefficient
K	Reaction rate coefficient for inhibition term
$\mathbf{K_p}$	Equilibrium constant for NO oxidation
$\mathbf{k_{ref}}$	Centered reaction rate coefficient
L	Loading matrix
M	Data matrix
n	Number of data points used for residual calculation
p	Parameter vector
P	Pressure
$\mathbf{p_A}$	Parameter value for A tuning

$\mathbf{p_{D,scale}}$	Parameter value for $f_{D,scale}$ tuning
$\mathbf{p_{Ea}}$	Parameter value for E_A tuning
r	Reaction rate
R	Ideal gas constant
res	Residual
S	Residual sum of squares
T	Temperature
$\mathbf{T_{ref}}$	Reference temperature
$\mathbf{T_s}$	Solid temperature
$\mathbf{w_A}$	Parameter weight factor for A
$\mathbf{w_{D,scale}}$	Parameter weight factor for $f_{D,scale}$
$\mathbf{w_{Ea}}$	Parameter weight factor for E_A
x	Variables vector
X	Mean absolute conversion
y	Mole fraction
$\mathbf{y_{model}}$	Simulated response
$\mathbf{y_{observed}}$	Observed response
z	Residual function
$\mathbf{\Delta H_{net}}$	Overall enthalpy change for NO oxidation reaction
$\mathbf{\Delta S_{net}}$	Overall entropy change for NO oxidation reaction

SUPERSCRIPTS AND INDEXES

i	Component
j	Reaction number
k	Segment (axial tank)
o	Original parameter value
T	Transposed

BIBLIOGRAPHY

1. Heck, R.M. and R.J. Farrauto, *Automobile exhaust catalysts.* Applied Catalysis A: General, 2001. **221**(1–2): p. 443-457.
2. Stone, R., *Introduction to internal combustion engines / Richard Stone*. 1992, Houndmills, Basingstoke [England] :: Macmillan.
3. Thom, S.R., *Hyperbaric-Oxygen Therapy for Acute Carbon Monoxide Poisoning.* New England Journal of Medicine, 2002. **347**(14): p. 1105-1106.
4. Kao, L. and K. Nanagas, *Toxicity associated with carbon monoxide.* Clinics in Laboratory Medicine, 2006. **26**: p. 28.
5. Pârvulescu, V.I., P. Grange, and B. Delmon, *Catalytic removal of NO.* Catalysis Today, 1998. **46**(4): p. 233-316.
6. (ARB), C.A.R.B., *Findings of the Scientific Review Panel On The Report on Diesel Exhaust*. 1998.
7. de Kok, T.M.C.M., et al., *Toxicological assessment of ambient and traffic-related particulate matter: A review of recent studies.* Mutation Research/Reviews in Mutation Research, 2006. **613**(2–3): p. 103-122.
8. Heck, R.M., R.J. Farrauto, and S.T. Gulati, *Catalytic air pollution control: Commercial technology, 2nd edition.* Environmental Progress, 2002. **21**(4): p. 141-161.
9. GmbH, N. *Precious Metal-Coated Substrates (e.g. Diesel Oxidation Converters)*. 2015 [cited 2015 0312]; Available from: http://www.namos.de/catalysis/index.php?doc=technologie&type=..
10. Chorkendorff, I. and J.W. Niemantsverdriet, *Concepts of modern catalysis and kinetics*. 2003: Wiley-VCH.
11. Auvray, X., *Fundamental studies of catalytic systems for diesel emission control*, in *Institutionen för kemi- och bioteknik, Kemisk reaktionsteknik, Chalmers tekniska högskola,*. 2013: Göteborg.
12. van Setten, B., M. Makkee, and J. Moulijn, *Science and technology of catalytic diesel particulate filters.* CATALYSIS REVIEWS-SCIENCE AND ENGINEERING, 2001. **43**: p. 76.
13. Nova, I., et al., *NH3–NO/NO2 chemistry over V-based catalysts and its role in the mechanism of the Fast SCR reaction.* Catalysis Today, 2006. **114**(1): p. 3-12.
14. Hogg, R., *Life beyond Euro VI*, in *Automotive Megatrends Magazine*. 2014, AW Megatrends Ltd: Penarth, UK. p. 2.
15. Voltz, S.E., et al., *Kinetic Study of Carbon Monoxide and Propylene Oxidation on Platinum Catalysts.* Product R&D, 1973. **12**(4): p. 294-301.
16. Lundstedt, T., et al., *Experimental design and optimization.* Chemometrics and Intelligent Laboratory Systems, 1998. **42**(1–2): p. 3-40.
17. Montgomery, D.C., *Design and Analysis of Experiments (7th Edition)*. 2009, John Wiley & Sons. p. 417-439.
18. Berger, R.J., et al., *Dynamic methods for catalytic kinetics.* Applied Catalysis A: General, 2008. **342**(1–2): p. 3-28.
19. Buzzi-Ferraris, G. and F. Manenti, *Kinetic models analysis.* Chemical Engineering Science, 2009. **64**(5): p. 1061-1074.
20. Martens, H. and T. Naes, *Multivariate Calibration*. 1989: John Wiley & Sons.

21. Olsson, I.-M., J. Gottfries, and S. Wold, *D-optimal onion designs in statistical molecular design.* Chemometrics and Intelligent Laboratory Systems, 2004. **73**(1): p. 37-46.
22. Olsson, I.-M., J. Gottfries, and S. Wold, *Controlling coverage of D-optimal onion designs and selections.* Journal of Chemometrics, 2004. **18**(12): p. 548-557.
23. Dieselnet. *Swedish Diesel Fuel Specifications*. 2013 [cited 2013 0215]; Available from: http://www.dieselnet.com/standards/se/fuel.php.
24. Kolaczkowski, S., et al., *Transient experiments on a full-scale DOC—Methodology and techniques to support modelling.* Catalysis Today, (0).
25. Sjoblom, J., *Bridging the gap between lab scale and full scale catalysis experimentation, in Capoc 2012.* Accepted for publication in Catalysis Today, 2012.
26. Kumar, A. and S. Mazumder, *Toward simulation of full-scale monolithic catalytic converters with complex heterogeneous chemistry.* Computers & Chemical Engineering, 2010. **34**(2): p. 135-145.
27. Štěpánek, J., et al., *Catalyst simulations based on coupling of 3D CFD tool with effective 1D channel models.* Catalysis Today, 2012. **188**(1): p. 87-93.
28. Stamatelos, A.M., et al., *Computer aided engineering in diesel exhaust aftertreatment systems design.* Proceedings of the Institution of Mechanical Engineers, Part D (Journal of Automobile Engineering), 1999. **213**(Copyright 2000, IEE): p. 545-60.
29. Güthenke, A., et al., *Current status of modeling lean exhaust gas aftertreatment catalysts*, in *Advances in Chemical Engineering*, G.B. Marin, Editor. 2007, Academic Press. p. 103-283.
30. Metkar, P.S., M.P. Harold, and V. Balakotaiah, *Experimental and kinetic modeling study of NH3-SCR of NOx on Fe-ZSM-5, Cu-chabazite and combined Fe- and Cu-zeolite monolithic catalysts.* Chemical Engineering Science, 2013. **87**(0): p. 51-66.
31. Ericson C, W.B., Odenbrand I, *A state-space simplified SCR catalyst model for real time applications.* SAE SP, NUMB 2155, 2008: p. 7.
32. Mladenov, N., et al., *Modeling of transport and chemistry in channel flows of automotive catalytic converters.* Chemical Engineering Science, 2010. **65**(2): p. 812-826.
33. Tronconi, E. and P. Forzatti, *Adequacy of Lumped Parameter Models for SCR Reactors with Monolith Structure.* Aiche Journal, 1992. **38**(2): p. 201-210.
34. Hawthorn, R.D., *Afterburner catalysts-effects of heat and mass transfer between gas and catalyst surface.* AIChE Symp. Ser., 1974. **70**: p. 11.
35. Fogler, H.S., *Elements of chemical reaction engineering*. Prentice Hall international series in the physical and chemical engineering sciences, ed. ed. 2006, Upper Saddle River, N.J.: Prentice Hall/PTR.
36. Lafossas, F., et al., *Calibration and Validation of a Diesel Oxidation Catalyst Model: from Synthetic Gas Testing to Driving Cycle Applications.* 2011.
37. Ansell, G.P., et al., *The development of a model capable of predicting diesel lean NOx catalyst performance under transient conditions.* Applied Catalysis B: Environmental, 1996. **10**(1-3): p. 183-201.
38. Watling, T.C., et al., *Development and Validation of a Pt-Pd Diesel Oxidation Catalyst Model.* SAE Technical Paper Number: 2012-01-1286, 2012.

39. Crocoll, M., S. Kureti, and W. Weisweiler, *Mean field modeling of NO oxidation over Pt/Al2O3 catalyst under oxygen-rich conditions.* Journal of Catalysis, 2005. **229**(2): p. 480-489.
40. Olsson, L., et al., *Mean field modelling of NOx storage on Pt/BaO/Al2O3.* Catalysis Today, 2002. **73**(3-4): p. 263-270.
41. Salomons, S., et al., *CO and H2 oxidation on a platinum monolith diesel oxidation catalyst.* Catalysis Today, 2006. **117**(4): p. 491-497.
42. Oh, S.H. and J.C. Cavendish, *Transients of monolithic catalytic converters. Response to step changes in feedstream temperature as related to controlling automobile emissions.* Industrial & Engineering Chemistry Product Research and Development, 1982. **21**(1): p. 29-37.
43. Wang, T.J., S.W. Baek, and J.H. Lee, *Kinetic parameter estimation of a diesel oxidation catalyst under actual vehicle operating conditions.* Industrial & Engineering Chemistry Research, 2008. **47**(8): p. 2528-2537.
44. Pandya, A., et al., *Global kinetic model and parameter optimization for a diesel oxidation catalyst.* Topics in Catalysis, 2009. **52**(13-20): p. 1929-1933.
45. Kandylas, I.P. and G.C. Koltsakis, *NO2-Assisted Regeneration of Diesel Particulate Filters: A Modeling Study.* Industrial & Engineering Chemistry Research, 2002. **41**(9): p. 2115-2123.
46. Guojiang, W. and T. Song, *CFD simulation of the effect of upstream flow distribution on the light-off performance of a catalytic converter.* Energy Conversion and Management, 2005. **46**(13–14): p. 2010-2031.
47. Tsinoglou, D.N. and G.C. Koltsakis, *Effect of perturbations in the exhaust gas composition on three-way catalyst light off.* Chemical Engineering Science, 2003. **58**(1): p. 179-192.
48. Koltsakis, G.C. and A.M. Stamatelos, *Modeling dynamic phenomena in 3-way catalytic converters.* Chemical Engineering Science, 1999. **54**(20): p. 4567-4578.
49. Dubien, C., et al., *Three-way catalytic converter modelling: fast- and slow-oxidizing hydrocarbons, inhibiting species, and steam-reforming reaction.* Chemical Engineering Science, 1998. **53**(3): p. 471-481.
50. Koltsakis, G.C., P.A. Konstantinidis, and A.M. Stamatelos, *Development and application range of mathematical models for 3-way catalytic converters.* Applied Catalysis B: Environmental, 1997. **12**(2–3): p. 161-191.
51. Chen, D.K.S., et al., *A Three-Dimensional Model for the Analysis of Transient Thermal and Conversion Characteristics of Monolithic Catalytic Converters*. 1988, SAE International, Technical Paper number. 880282.
52. Olsson, L., et al., *A Kinetic Study of Oxygen Adsorption/Desorption and NO Oxidation over Pt/Al2O3 Catalysts.* The Journal of Physical Chemistry B, 1999. **103**(47): p. 10433-10439.
53. Irani, K., W.S. Epling, and R. Blint, *Effect of hydrocarbon species on no oxidation over diesel oxidation catalysts.* Applied Catalysis B: Environmental, 2009. **92**(3–4): p. 422-428.
54. Tronconi, E. and A. Beretta, *The role of inter- and intra-phase mass transfer in the SCR-DeNO(x) reaction over catalysts of different shapes.* Catalysis Today, 1999. **52**(2-3): p. 249-258.
55. Sjoblom, J. and D. Creaser, *Latent variable projections of sensitivity data for experimental screening and kinetic modeling.* Computers & Chemical Engineering, 2008. **32**(12): p. 3121-3129.

56. Box, G.E.P., et al., *Some Problems Associated with the Analysis of Multiresponse Data.* Technometrics, 1973. **15**(1): p. 33-51.
57. Hauff, K., et al., *A global description of DOC kinetics for catalysts with different platinum loadings and aging status.* Applied Catalysis B: Environmental, 2010. **100**(1–2): p. 10-18.
58. Froment, G.F., J. De Wilde, and K.B. Bischoff, *Chemical reactor analysis and design*. Vol. 3rd ed. 2011, Hoboken, N.J: Wiley.
59. Coleman, T.F. and Y.Y. Li, *An interior trust region approach for nonlinear minimization subject to bounds.* Siam Journal on Optimization, 1996. **6**(2): p. 418-445.
60. Metkar, P.S., et al. *Kinetics and mechanistic studies of selective catalytic reduction of NOx on fe based zeolite monolith catalysts*. 2010.
61. Nova, I., et al., *Influence of the Substrate Properties on the Performances of NH3-SCR Monolithic Catalysts for the Aftertreatment of Diesel Exhaust: An Experimental and Modeling Study.* Industrial & Engineering Chemistry Research, 2010. **50**(1): p. 299-309.
62. Wickman, B., et al., *Modeling mass transport with microkinetics in monolithic NO x storage and reduction catalyst.* Topics in Catalysis, 2007. **42-43**(1-4): p. 123-127.